Global convergence and quasi-reversibility for a coefficient inverse problem with backscattering data

Andrey V. Kuzhuget,* Larisa Beilina,† Michael V. Klibanov, ‡ and Vladimir G. Romanov. §

Abstract

A globally convergent numerical method is developed for a 2-d Coefficient Inverse Problem for a hyperbolic PDE with the backscattering data. An important part of this technique is the quasi-reversibility method. A global convergence theorem is proven via a Carleman estimate. Results of numerical experiments for the problem modeling imaging of plastic land mines are presented.

KEY WORDS: inverse problems, globally convergent method, quasi-reversibility method, Carleman estimate

AMS subject classification: 15A15, 15A09, 15A23

1 Introduction

In this work we extend the recently developed globally convergent numerical method of [1, 2, 3, 4] for a hyperbolic Coefficient Inverse Problem (CIP) for the case of backscattering data. Note that only the case of the data given at the entire boundary was considered [1, 2, 3, 4]. Just as before, we work with a CIP with the data resulting from a single measurement, i.e. either a single position of the point source or a single direction of the initializing plane wave. Since we have both Dirichlet and Neumann boundary conditions on the backscattering part of the boundary of the domain of interest, we use the Quasi-Reversibility Method (QRM) [15], which was not a part of [1, 2, 3, 4]. We refer to, e.g. [5, 6, 8, 13, 14] for some recent publications on the QRM.

*Department of Mathematics and Statistics, University of North Carolina at Charlotte, Charlotte, NC 28223, USA (akuzhuge@uncc.edu).

†Department of Mathematical Sciences, Chalmers University of Technology and Gothenburg University, SE-42196 Gothenburg, Sweden, (larisa@chalmers.se).

‡Department of Mathematics and Statistics, University of North Carolina at Charlotte, Charlotte, NC 28223, USA (mklibanv@uncc.edu).

§Sobolev Mathematical Institute of the Siberian Branch of the Russian Academy of Sciences, Koptyug Prospect 2, Novosibirsk 630090, Russia (romanov@math.nsc.ru).

The main new analytical result here is the proof of the global convergence theorem in the case when the QRM is used. To do so, we first obtain an analog of *a priori* upper estimate of the QRM solution using a Carleman estimate. Next, the global convergence result is established. Applications of our CIP are in imaging of dielectric constants of explosives, since their dielectric constants are much higher than those of regular materials, see http://www.clippercontrols.com/info/. The target application of this publication is in imaging of plastic land mines. We also mention an important application of CIPs with backscattering data to geophysics.

We point out that an independent verification of the technique of [1] was carried out in [12] for the case of experimental data. Computations were conducted for *blind* data only. Comparison of computed refractive indices of dielectric abnormalities with *a posteriori* measured ones has revealed an excellent accuracy of computational results. Because of this accuracy, it was concluded in [12] that the technique of [1, 2] "is completely validated now", regardless on a certain approximation, which is a part of that technique. This conclusion justifies the same approximation of the current paper. In our opinion, some approximation like this one are inevitable for such challenging problems as CIPs are. Indeed, CIPs are both nonlinear and ill-posed.

That approximation is due to the truncation of certain Volterra-like integrals at a high value $\overline{s} > 1$ of the parameter $s > 0$ of the Laplace transform of the original hyperbolic PDE. We call s *pseudo frequency*. This truncation is similar with the truncation of high frequencies. As an analogy, we point out that such truncations are routinely done in engineering without any proofs of convergence, and still those things usually work quite well in practice. The meaning of this approximation was discussed in detail in subsection 3.3 of [12] and in subsection 6.3 of [2], where a new mathematical model was proposed. In particular, it was shown in these references that this model has the same nature as the truncation of divergent asymptotic series in the classical Real Analysis.

We use a two-stage numerical procedure here, the framework of which was developed in [2, 3, 4]. Indeed, because of the above approximation, the global convergence theorem only guarantees that the resulting solution is sufficiently close to the correct one. However, it does not guarantee that this solution can be made infinitely close to the correct one, because the truncation pseudo frequency $\overline{s}$ cannot be made infinitely large in practical computations. On the other hand, the availability of a good first approximation for the correct solution is the *key component* of any locally convergent algorithm. Therefore, our procedure works as follows. On the first stage the globally convergent numerical method provides a good first approximation for the solution. On the second stage this approximation is refined via a locally convergent modified gradient method, which uses the solution of the first stage as its starting point.

More precisely, our numerical experience shows that the first stage provides good locations of mine-like targets. The subsequent application of the second stage, which is a modified gradient method in our case, provides accurate values of the unknown coefficient within those targets. At the same time, it is worthy to note that the modified gradient method being applied without the first stage results in quite inaccurate images (not shown here), even if

the background value of the unknown coefficient is taken as the starting point, see subsection 8.4 of [12] for a similar observation.

In section 2 we formulate both forward and inverse problems. In section 3 we formulate the layer stripping procedure with respect to s. In section 4 we describe the algorithm. New analytical results are presented in sections 5 and 6. In section 5 estimates for solutions resulting from the QRM are derived. The global convergence theorem is proven in section 6. In section 7 a simplified mathematical model of imaging of land mines is formulated. In section 8 results of numerical studies are presented.

2 Statements of Forward and Inverse Problems

We work with the 2-d case only. Some properties of the solution of the forward problem were established in the 3-d case in [3]. Their extensions to the 2-d case can be done along the same lines, although it is space consuming. Hence, for brevity we use these properties here, assuming that they hold for 2-d.

Denote $\mathbf{x} = (x, z) \in \mathbb{R}^2$. As the forward problem, we consider the Cauchy problem for a hyperbolic PDE

$$c(\mathbf{x})\, u_{tt} = \Delta u \text{ in } \mathbb{R}^2 \times (0, \infty), \tag{2.1}$$

$$u(\mathbf{x}, 0) = 0, u_t(\mathbf{x}, 0) = \delta(\mathbf{x} - \mathbf{x}_0). \tag{2.2}$$

Equation (2.1) governs, e.g. propagation of acoustic and electromagnetic waves. In the acoustical case $1/\sqrt{c(\mathbf{x})}$ is the sound speed. In the 2-d case of EM waves propagation in a non-magnetic medium the coefficient $c(\mathbf{x})$ is $c(\mathbf{x}) := \varepsilon_r(\mathbf{x})$, where $\varepsilon_r(\mathbf{x})$ is the spatially distributed dielectric constant, i.e. $\varepsilon_r(\mathbf{x}) = \varepsilon(\mathbf{x})/\varepsilon_0$, where $\varepsilon(\mathbf{x})$ is the spatially distributed electric permittivity of the medium and ε_0 is the dielectric permittivity of the vacuum, see [7] for the derivation of (2.1) from Maxwell's equations in the 2-d case. Let $\Omega \subset \mathbb{R}^2$ be a convex bounded domain with the piecewise smooth boundary $\partial\Omega$. As it is always the case of the QRM, we need to assume a certain over-smoothness of the solution. So, we assume that the function $c(\mathbf{x})$ satisfies the following conditions

$$c(\mathbf{x}) \geq 1, c(\mathbf{x}) = 1 \text{ for } \mathbf{x} \in \mathbb{R}^2 \setminus \Omega, \tag{2.3}$$

$$c(\mathbf{x}) \in C^4\left(\mathbb{R}^2\right). \tag{2.4}$$

We will work with the Laplace transform of the functions u,

$$w(\mathbf{x}, s) = \int_0^\infty u(\mathbf{x}, t) e^{-st} dt, \text{ for } s \geq \underline{s} = const. > 0, \tag{2.5}$$

where $\underline{s}$ is a certain number. In our numerical studies we choose $\underline{s}$ experimentally. We call the parameter s *pseudo frequency*. Equation for the function w is

$$\Delta w - s^2 c(\mathbf{x})\, w = -\delta(\mathbf{x} - \mathbf{x}_0), \forall s \geq \underline{s}, \tag{2.6}$$

$$\lim_{|\mathbf{x}| \to \infty} w(\mathbf{x}, s) = 0, \forall s \geq \underline{s}. \tag{2.7}$$

The condition (2.7) was established in [3] for sufficiently large values of $\underline{s}$. In addition, for these values of $\underline{s}$ [3]

$$w(\mathbf{x}, s) > 0. \tag{2.8}$$

In the course of the proof of the convergence theorem (section 6) we will work with functions $c \in C^1(\mathbb{R}^2) \subset C^\gamma(\mathbb{R}^2), \forall \gamma \in (0,1)$. Below $C^{k+\gamma}$ are Hölder spaces, where $k \geq 0$ is an integer. It follows from the classic theory of elliptic PDEs [11] that if $c \in C^{k+\gamma}(\mathbb{R}^2)$, then $w \in C^{k+2+\gamma}(\mathbb{R}^2 \setminus \{|x - x_0| < \theta\}), \forall \theta > 0$.

In our derivations we need an asymptotic behavior of the function $w(\mathbf{x}, s)$ at $s \to \infty$, which is formulated in Lemma 2.1. Although this lemma is now formulated only for the 3-d case, we assume that it is valid in the 2-d case as well, see the beginning of this section.

Lemma 2.1 [1]. *Assume that conditions (2.3) and (2.4) are satisfied and that we work in* $\mathbb{R}^3$. *Let the function* $w(\mathbf{x}, s) \in C^{5+\gamma}(\mathbb{R}^3 \setminus \{|\mathbf{x} - \mathbf{x}_0| < \theta\}), \forall \theta > 0$ *be the solution of the problem (2.6), (2.7). Assume that geodesic lines, generated by the eikonal equation corresponding to the function* $c(\mathbf{x})$ *are regular, i.e. any two points in* $\mathbb{R}^3$ *can be connected by a single geodesic line. Let* $l(\mathbf{x}, \mathbf{x}_0)$ *be the length of the geodesic line connecting points* $\mathbf{x}$ *and* $\mathbf{x}_0$. *Then the following asymptotic behavior of the function* w *and its derivatives takes place for* $|\alpha| \leq 2, k = 0, 1, \mathbf{x} \neq \mathbf{x}_0$

$$D_{\mathbf{x}}^{\alpha} D_s^k w(\mathbf{x}, s) = D_{\mathbf{x}}^{\alpha} D_s^k \left\{ \frac{\exp[-sl(\mathbf{x}, \mathbf{x}_0)]}{f(\mathbf{x}, \mathbf{x}_0)} \left[1 + O\left(\frac{1}{s}\right) \right] \right\}, s \to \infty, \tag{2.9}$$

where $f(\mathbf{x}, \mathbf{x}_0)$ *is a certain function and* $f(\mathbf{x}, \mathbf{x}_0) \neq 0$ *for* $\mathbf{x} \neq \mathbf{x}_0$.

An interesting question here is about an easily verifiable sufficient condition of the regularity of geodesic lines. In general, such a condition is unknown, except of the trivial case when the function $c(\mathbf{x})$ is close to a constant. To our best knowledge, the only case of such a condition in 2-d is

$$\Delta \ln c(\mathbf{x}) \geq 0, \forall \mathbf{x} \in \mathbb{R}^2,$$

see [17] as well as Theorem 2 in Chapter 2 of [9]. However, this condition is not satisfied in our computational examples. So, we verify (2.9) numerically in our computations (subsection 7.2 of [1]): this is a typical case when the computational experience is less pessimistic than the theory. Thus, everywhere below we assume that the asymptotic behavior (2.9) is valid.

To simplify the presentation and also because of our target application to imaging of plastic land mines, we now specify the domain $\Omega \subset \mathbb{R}^2$. Let $B > 0$ be a constant. Below

$$\Omega = (-B, B) \times (0, 2B), \partial\Omega = \cup_{i=1}^4 \Gamma_i, \tag{2.10a}$$

$$\Gamma_1 = \partial\Omega \cap \{z = 0\}, \Gamma_2 = \partial\Omega \cap \{x = B\}, \tag{2.10b}$$

$$\Gamma_3 = \partial\Omega \cap \{x = -B\}, \Gamma_4 = \partial\Omega \cap \{z = 2B\}. \tag{2.10c}$$

Inverse Problem. *Suppose that the coefficient* $c(\mathbf{x})$ *in equation (2.6) satisfies conditions (2.3), (2.4) and is unknown in the domain* Ω. *Determine the function* $c(\mathbf{x})$ *for* $\mathbf{x} \in \Omega$, *assuming that the following functions* $\varphi_0(x, s)$ *and* $\varphi_1(x, s)$ *are known for a single source position* $\mathbf{x}_0 \notin \overline{\Omega}$

$$w(\mathbf{x}, s)|_{\Gamma_1} = \varphi_0(x, s), w_z(\mathbf{x}, s)|_{\Gamma_1} = \varphi_1(x, s), \forall s \in [\underline{s}, \overline{s}], \tag{2.11}$$

where $\overline{s} > \underline{s}$ is a number, which should be chosen experimentally in numerical studies.

Note that in experiments usually only the function $u(x,0,t)$ is measured. One can approximately assume that the function $u(x,0,t)$ is known for all $x \in \mathbb{R}$ implying that the function $\varphi_0(x,s)$ is known for all $x \in \mathbb{R}$ and for all $s \in [\underline{s}, \overline{s}]$ via the Laplace transform (2.5) of $u(x,0,t)$. Next, since the coefficient $c(\mathbf{x}) = 1$ is known for $z < 0$, then solving the forward problem (2.6), (2.7) in the half plane $\{z < 0\}$ with the boundary condition $w(x,0,s) = \varphi_0(x,s)$, one can uniquely determine the function $w(\mathbf{x},s)$ for $z < 0$, thus coming up with the function $w_z(x,0,s) = \varphi_1(x,s)$.

The question of uniqueness of this CIP is a well known long standing problem. Currently it can be addressed positively via the method of Carleman estimates only in the case when the $\delta(\mathbf{x} - \mathbf{x}_0)$ in (2.2) is replaced with such a function $f(\mathbf{x})$ that $f(\mathbf{x}) \neq 0$ in $\overline{\Omega}$ [13]. Nevertheless, the authors believe that, because of the applied aspect, it makes sense to develop a globally convergent method for this CIP, assuming that uniqueness holds.

3 Layer Stripping With Respect to s

By (2.8) we can consider the function $v = \ln w / s^2$. Hence, (2.6) and (2.11) lead to

$$\Delta v + s^2 |\nabla v|^2 = c(\mathbf{x}), \quad \mathbf{x} \in \Omega, \tag{3.1}$$

$$v|_{\Gamma_1} = \varphi_2(x,s), \quad v_z|_{\Gamma_1} = \varphi_3(x,s), \ \forall s \in [\underline{s}, \overline{s}], \tag{3.2}$$

where $\varphi_2 = \ln \varphi_0 / s^2, \varphi_3 = \varphi_1 / (s^2 \varphi_0)$. The term $\delta(\mathbf{x} - \mathbf{x}_0)$ is not present in (3.1) because $\mathbf{x}_0 \notin \overline{\Omega}$. We now eliminate the function $c(\mathbf{x})$ from equation (3.1) via the differentiation with respect to s, since $\partial_s c(\mathbf{x}) = 0$. Introduce a new function $q(\mathbf{x},s) = \partial_s v(\mathbf{x},s)$. Lemma 2.1 implies that

$$D^\alpha_{\mathbf{x}}(v) = O\left(\frac{1}{s}\right), D^\alpha_{\mathbf{x}}(q) = O\left(\frac{1}{s^2}\right), s \to \infty; |\alpha| \leq 2, \tag{3.3}$$

$$v(\mathbf{x},s) = -\int_s^\infty q(\mathbf{x},\tau)\, d\tau. \tag{3.4}$$

We truncate the integral in (3.4) as

$$v(\mathbf{x},s) \approx -\int_s^{\overline{s}} q(\mathbf{x},\tau)\, d\tau, \tag{3.5}$$

where $\overline{s} > \underline{s}$ is a large parameter which should be chosen in numerical experiments. Actually, $\overline{s}$ is one of regularization parameters of our method. In fact, we have truncated here the function $V(\mathbf{x},\overline{s})$, which we call the *tail function*,

$$V(\mathbf{x},\overline{s}) = -\int_{\overline{s}}^\infty q(\mathbf{x},\tau)\, d\tau.$$

By (3.3)

$$\left\| D_{\overline{s}}^{k} V\left(\mathbf{x}, \overline{s}\right) \right\|_{C^2\left(\overline{\Omega}\right)} = O\left(\frac{1}{\overline{s}^{k+1}}\right), k = 0, 1;\ \overline{s} \to \infty. \tag{3.6}$$

Although by (3.6) the tail is small for the large values of $\overline{s}$, the numerical experience of [1, 2, 3, 4, 12] shows one should that it would be better to somehow approximate the tail function updating it via an iterative procedure.

Thus, still taking into account the tail, we obtain from (3.1) and (3.5) the following nonlinear integral differential equation

$$\begin{aligned} &\Delta q - 2s^2 \nabla q \cdot \int_s^{\overline{s}} \nabla q\left(x, \tau\right) d\tau + 2s \left[\int_s^{\overline{s}} \nabla q\left(x, \tau\right) d\tau \right]^2 \\ &+ 2s^2 \nabla q \nabla V - 2s \nabla V \cdot \int_s^{\overline{s}} \nabla q\left(x, \tau\right) d\tau + 2s \left(\nabla V\right)^2 = 0. \end{aligned} \tag{3.7}$$

Let $\psi_0\left(x, s\right) = \partial_s \varphi_2\left(x, s\right), \psi_1\left(s\right) = \partial_s \varphi_3\left(x, s\right)$. Then (3.2) implies that

$$q|_{\Gamma_1} = \psi_0\left(x, s\right), q_z|_{\Gamma_1} = \psi_1\left(x, s\right),\ \forall s \in \left[\underline{s}, \overline{s}\right]. \tag{3.8}$$

A slight modification of arguments of subsection 2.2 of [3] shows that, for if $s > \underline{s}$ and $\underline{s}$ is sufficiently large, then the function $w\left(\mathbf{x}, s\right)$ tends to zero together with its appropriate $\left(\mathbf{x}, s\right)-$derivatives as $|\mathbf{x}| \to \infty$ (in both 3-d and 2-d cases), which is slightly more general than (2.7). Hence, we have the following radiation condition

$$\lim_{B \to \infty} \left(\frac{\partial w}{\partial \nu_i} + sw \right) |_{\Gamma_i} = 0, i = 2, 3, 4.$$

where ν_i is the outer normal vector on Γ_i. Since $q(\mathbf{x}, s) = \partial_s \left(s^{-2} \ln w\right)$, then we obtain from the latter the following approximate Neumann boundary condition for the function q at Γ_i

$$\partial_{\nu_i} q\ |_{\Gamma_i} = s^{-2},\ i = 2, 3, 4. \tag{3.9}$$

So, while conditions (3.8) change with the change of the unknown coefficient $c\left(\mathbf{x}\right)$, the condition (3.9) is generic and it is independent on $c\left(\mathbf{x}\right)$. Thus, we use conditions (3.9) only to stabilize the problem.

The presence of integrals in (3.7) implies the nonlinearity, which is the main difficulty here. If the functions q and V are approximated well from (3.7)-(3.9) together with their $\mathbf{x}-$derivatives up to the second order, then the target unknown coefficient $c\left(\mathbf{x}\right)$ is also approximated well from (3.1), where the function v is computed from (3.5), where the function V is added. Thus, below we focus on the following question: *How to solve numerically the problem (3.7)-(3.9)?*

Remark 3.1. Since the tail function V is unknown, equation (3.7) contains two unknown functions q and V. The reason why we can approximate both of them is that we treat them

differently: while we approximate the function q via inner iterations, the function V is approximated via outer iterations.

We approximate the function $q(\mathbf{x}, s)$ as a piecewise constant function with respect to the pseudo frequency s. That is, we assume that there exists a partition $\underline{s} = s_N < s_{N-1} < ... < s_1 < s_0 = \overline{s}$ of the interval $[\underline{s}, \overline{s}]$ with the sufficiently small grid step size $h = s_{i-1} - s_i$ such that $q(\mathbf{x}, s) = q_n(\mathbf{x})$ for $s \in (s_n, s_{n-1}]$. We approximate the boundary condition (3.8), (3.9) as

$$q_n|_{\Gamma_1} = \overline{\psi}_{0,n}(x),\ \partial_z q_n|_{\Gamma_1} = \overline{\psi}_{1,n}(x),\ \partial_\nu q_n|_{\Gamma_i} = (s_n s_{n-1})^{-1}, i = 2, 3, 4. \tag{3.10}$$

where $\overline{\psi}_{0,n}$, $\overline{\psi}_{1,n}$ and $(s_n s_{n-1})^{-1}$ are averages of functions ψ_0, ψ_1 and s^{-1} over the interval (s_n, s_{n-1}). Rewrite (3.7) for $s \in (s_n, s_{n-1}]$ using this piecewise constant approximation. Then multiply the resulting approximate equation by the s-dependent Carleman Weight Function (CWF) of the form

$$\mathcal{C}_{n,\mu}(s) = \exp\left[-\mu\left|s - s_{n-1}\right|\right], s \in (s_n, s_{n-1}],$$

and integrate with respect to $s \in (s_n, s_{n-1}]$. We obtain the following approximate equation in Ω for the function $q_n(\mathbf{x}), n = 1, ..., N$

$$\begin{aligned} L_n(q_n) &:= \Delta q_n - A_{1n}\left(h\sum_{j=1}^{n-1}\nabla q_j - \nabla V_n\right)\nabla q_n = \\ &= B_n(\nabla q_n)^2 - A_{2,n}h^2\left(\sum_{j=1}^{n-1}\nabla q_j\right)^2 + 2A_{2,n}\nabla V_n\left(h\sum_{j=1}^{n-1}\nabla q_j\right) - A_{2,n}(\nabla V_n)^2. \end{aligned} \tag{3.11}$$

We have intentionally inserted dependence of the tail function V_n from the iteration number n here because we will approximate these functions iteratively. In (3.11) $A_{1,n} = A_{1,n}(\mu, h)$, $A_{2,n} = A_{2,n}(\mu, h), B_n = B_n(\mu, h)$ are certain numbers depending on μ and h, see specific formulas in [1]. It is convenient to set in (3.11)

$$q_0 \equiv 0. \tag{3.12}$$

Since boundary value problems (3.10), (3.11) are actually generated by equation (3.7), which contains Volterra-like s-integrals, then these problems can be solved sequentially starting from q_1. Since boundary conditions (3.10) are over-determined ones, it is natural to apply a version of the QRM here, because the QRM finds "least squares" solutions in the case of over-determined boundary conditions.

Remark 3.2. As to (3.11), an important point is that $|B_n(\mu, h)| \leq 8\overline{s}^2/\mu$ for $\mu h \geq 1$ [1]. We have used $\mu = 50$ in our computations. Hence, assuming that $\mu >> 1$,we ignore the nonlinear term in (3.11) below via setting $B_n(\nabla q_n)^2 := 0$. This allows us to solve a linear problem for each q_n.

4 The Algorithm

Our algorithm reconstructs iterative approximations $c_{n,k}(\mathbf{x}) \in C^1\left(\overline{\Omega}\right)$ of the function $c(\mathbf{x})$. On the other hand, to iterate with respect to the tails, we need to solve the forward problem

(2.6), (2.7) in $\mathbb{R}^2$ on each iterative step. To do this, we extend each function $c_{n,k}(\mathbf{x})$ outside of the Ω, so that the resulting function $\widehat{c}_{n,k}(\mathbf{x}) = 1$ outside of $\Omega, \widehat{c}_{n,k}(\mathbf{x}) = c_{n,k}(\mathbf{x})$ in a subdomain $\Omega' \subset\subset \Omega$ and $\widehat{c}_{n,k} \in C^1(\mathbb{R}^2)$. In addition, to ensure the ellipticity of the operator in (2.6), we need to have $\widehat{c}_{n,k}(\mathbf{x}) \geq const. > 0$ in $\mathbb{R}^2$. So, we now describe a rather standard procedure of such an extension. Choose a function $\chi(\mathbf{x}) \in C^\infty(\mathbb{R}^2)$ such that

$$\chi(\mathbf{x}) = \begin{cases} 1 \text{ in } \Omega', \\ \text{between 0 and 1 in } \Omega \diagdown \Omega', \\ 0 \text{ outside of } \Omega. \end{cases}$$

The existence of such functions $\chi(\mathbf{x})$ is well known from the Real Analysis course. Define the target extension of the function $c_{n,k}$ as $\widehat{c}_{n,k}(\mathbf{x}) := (1 - \chi(\mathbf{x})) + \chi(\mathbf{x}) c_{n,k}(\mathbf{x}), \forall x \in \mathbb{R}^2$. Hence, $\widehat{c}_{n,k}(\mathbf{x}) = 1$ outside of Ω and $\widehat{c}_{n,k} \in C^1(\mathbb{R}^2)$. Let $\widetilde{\Omega} \subseteq \Omega$ be a subdomain and $\Omega' \subset\subset \widetilde{\Omega}$. Suppose that $c_{n,k}(\mathbf{x}) \geq 1/2$ in $\widetilde{\Omega}$. Then $\widehat{c}_{n,k}(\mathbf{x}) \geq 1/2$ in Ω. Indeed, $\widehat{c}_{n,k}(\mathbf{x}) - 1/2 = (1 - \chi(\mathbf{x}))/2 + \chi(\mathbf{x})(c_{n,k}(\mathbf{x}) - 1/2) \geq 0$.

4.1 The iterative process

We now present our algorithm. On each iterative step n we approximate both the function q_n and the tail function V_n, see Remark 3.1. Each iterative step requires an approximate solution of the boundary value problem (4.10), (4.11). This is done via the QRM, which is described in subsection 4.2. First, we choose an initial tail function $V_{1,1}(\mathbf{x}) \in C^2(\overline{\Omega})$ and use (3.12). As to the choice of $V_{1,1}$, it was taken as $V_{1,1} \equiv 0$ in [1]. In later publications [2, 3, 4, 12] $V_{1,1}$ was taken as the one, which corresponds to the case $c(\mathbf{x}) \equiv 1$, where $c(\mathbf{x}) := 1$ is the value of the unknown coefficient outside of the domain of interest Ω, see (2.3). An observation was that while both these choices give the same result, the second choice leads to a faster convergence and both choices satisfy conditions of the global convergence theorem. For each q_n we have inner iterations with respect to tails.

Step n^k, where $n, k \geq 1$. Recall that by (3.12) $q_0 \equiv 0$. Suppose that functions $q_i \in H^5(\Omega), i = 1, ..., n-1$ and tails $V_1, ..., V_{n-1}, V_{n,k} \in C^2(\overline{\Omega})$ are constructed. To construct the function $q_{n.k}$, we use the QRM (subsection 4.2) to find an approximate solution of the following boundary value problem in Ω

$$\Delta q_{n,k} - A_{1n}\left(h\sum_{j=1}^{n-1}\nabla q_j - \nabla V_{n,k}\right)\nabla q_{n,k} =$$

$$-A_{2,n}h^2\left(\sum_{j=1}^{n-1}\nabla q_j\right)^2 + 2A_{2,n}\nabla V_{n,k}\cdot\left(h\sum_{j=1}^{n-1}\nabla q_j\right) - A_{2,n}\left(\nabla V_{n,k}\right)^2, \tag{4.1}$$

$$q_{n,k}|_{\Gamma_1} = \overline{\psi}_{0,n}(x),\ \partial_z q_{n,k}|_{\Gamma_1} = \overline{\psi}_{1,n}(x),\ \partial_{\nu_i} q_{n,k}|_{\Gamma_i} = (s_n s_{n-1})^{-1}, i = 2, 3, 4.$$

Hence, we obtain the function $q_{n,k} \in H^5(\Omega)$. By the embedding theorem $q_{n,k} \in C^3(\overline{\Omega})$. To reconstruct an approximation $c_{n,k}(\mathbf{x})$ for the function $c(\mathbf{x})$, we first, use (3.5) to calculate

an approximation for $v(\mathbf{x}, s_n)$ as

$$v_{n,k}(\mathbf{x}, s_n) = -hq_{n,k}(\mathbf{x}) - h\sum_{j=1}^{n-1} q_j(\mathbf{x}) + V_{n,k}(\mathbf{x}). \tag{4.2}$$

Next, using (3.1), we set for $n \geq 1$

$$c_{n,k}(\mathbf{x}) = \Delta v_{n,k}(\mathbf{x}, s_n) + s_n^2 \left|\nabla v_{n,k}(\mathbf{x}, s_n)\right|^2, \mathbf{x} \in \Omega. \tag{4.3}$$

Assuming that the exact solution of our Inverse Problem $c^* \geq 1$ in $\mathbb{R}^2$ (see (2.3)), it follows from Theorem 6.1 that $c_{n,k}(\mathbf{x}) \geq 1/2$ in $\Omega_\varkappa \subset \Omega$, where the subdomain $\Omega_\varkappa$ is defined in section 5. Next, we construct the function $\widehat{c}_{n,k}(\mathbf{x})$ as in the beginning of this section. Hence, by (4.1)-(4.3) the function $\widehat{c}_{n,k} \in C^\gamma(\mathbb{R}^2)$. Next, we solve the forward problem (2.6), (2.7) with $c(\mathbf{x}) := \widehat{c}_{n,k}(\mathbf{x})$ for $s := \overline{s}$ and obtain the function $w_{n.k}(\mathbf{x}, \overline{s})$. Next, we set for the new tail

$$V_{n,k+1}(\mathbf{x}) = \frac{\ln w_{n.k}(\mathbf{x}, \overline{s})}{\overline{s}^2} \in C^2\left(\overline{\Omega}\right).$$

We continue these iterations with respect to tails until convergence occurs. We cannot prove this convergence. However, we have always observed numerically that functions $q_{n,k}, c_{n,k}$ and $V_{n,k}$ have stabilized at $k := m$ for a certain m. So, assuming that they are stabilized, we set

$$c_n(\mathbf{x}) := c_{n,m}(\mathbf{x}), q_n(\mathbf{x}) := q_{n,m}(\mathbf{x}), V_n(\mathbf{x}) := V_{n,m}(\mathbf{x}) := V_{n+1,1}(\mathbf{x}) \text{ for } \mathbf{x} \in \Omega.$$

We stop iterations with respect to n at $n := N$.

4.2 The quasi-reversibility method

Let $H_{n,k}(\mathbf{x})$ be the right hand side of equation (4.1) for $n \geq 1$. Denote

$$a_{n,k}(\mathbf{x}) = A_{1,n}\left(h\sum_{j=1}^{n-1} \nabla q_j - \nabla V_{n,k}\right) \tag{4.4}$$

Then the boundary value problem (4.1) can be rewritten as

$$\Delta q_{n,k} - a_{n,k} \cdot \nabla q_{n,k} = H_{n,k}, \tag{4.5}$$

$$q_{n,k}|_{\Gamma_1} = \overline{\psi}_{0,n}(x),\ \partial_z q_{n,k}|_{\Gamma_1} = \overline{\psi}_{1,n}(x),\ \partial_{\nu_i} q_{n,k}|_{\Gamma_i} = (s_n s_{n-1})^{-1}, i = 2, 3, 4. \tag{4.6}$$

Since we have two boundary conditions rather then one at Γ_1, we find the "least squares" solution of the problem (4.5), (4.6) via the QRM. Specifically, we minimize the following Tikhonov functional

$$J_{n,k}^\alpha(u) = \|\Delta u - a_{n,k} \cdot \nabla u - H_{n,k}\|_{L_2(\Omega)}^2 + \alpha \|u\|_{H^5(\Omega)}^2, \tag{4.7}$$

subject to boundary condition (4.6), where the small regularization parameter $\alpha \in (0,1)$. Let $u(x)$ be the minimizer of this functional. Then we set $q_{n,k}(\mathbf{x}) := u(\mathbf{x})$. Local minima do not occur here because (4.7) is the sum of square norms of two expressions, both of which are linear with respect to u, also see Lemmata 5.2 and 5.3 in section 5. The second term in the right hand side of (4.7) is the Tikhonov regularization term. We use the $H^5(\Omega)-$norm here in order to ensure that the minimizer $u := q_{n,k} \in C^3\left(\overline{\Omega}\right)$, which implies in turn that functions $\widehat{c}_{n,k} \in C^1(\mathbb{R}^2)$.

Remarks 4.1. 1. In our computations we relax the smoothness assumptions via considering the $H^2(\Omega)-$norm in the second term in the right hand side of (4.7). This is possible because in computations we actually work with finite dimensional spaces. Specifically, we work with finite differences and do not use "overly fine" mesh, which means that dimensions of our "computational spaces" are not exceedingly large. In this case all norms are equivalent not only theoretically but practically as well. To the contrary, if the mesh would be too fine, then the corresponding space would be "almost" infinite dimensional.

2. One may pose a question on why we would not avoid the QRM via using just one of two boundary conditions at Γ_1 in (4.6), since we have the Neumann boundary condition at $\partial\Omega \diagdown \Gamma_1$. However, in this case we would be unable to prove the C^3- smoothness of the function $q_{n,k}$, because the boundary $\partial\Omega$ is not smooth. In the case of the Dirichlet boundary condition only $q_{n,k}|_{\Gamma_1}$ we would be unable to prove smoothness even assuming that $\partial\Omega \in C^\infty$, because of the Neumann boundary condition at the rest of the boundary. Besides, in our convergence estimate of the QRM in Theorem 5.1 we do not use the boundary condition (4.6) at Γ_4. Finally, since conditions $\partial_{\nu_i} q_{n,k}|_{\Gamma_i} = (s_n s_{n-1})^{-1}$ are independent on the target coefficient, it seems to be that two boundary conditions rather than one at Γ_1 should provide a better reconstruction.

5 Estimates for the QRM

For brevity we scale variables in such a way that in sections 5 and 6 $\Omega = (-1/4, 1/4) \times (0, 1/2)$. In sections 5 and 6 $C = C(\Omega) > 0$ denotes different positive constants depending only on the domain Ω. Let $\lambda, \nu > 2$ be two parameters. Introduce another Carleman Weight Function (CWF) $K(z)$,

$$K(z) := K_{\lambda,\nu}(z) = \exp(\lambda \rho^{-\nu}), \text{ where } \rho(z) = z + \frac{1}{4}, z > 0.$$

Note that $\rho(z) \in (0, 3/4)$ in Ω and $\rho(z)\,|_{\Gamma_4} = 3/4$. Let the number $\varkappa \in (1/3, 1)$. Denote $\Omega_\varkappa = \{\mathbf{x} \in \Omega : \rho(z) < 3\varkappa/4\}$. Hence, if $\varkappa_1 < \varkappa_2$, then $\Omega_{\varkappa_1} \subset\subset \Omega_{\varkappa_2}$. Also, $\Omega_1 = \Omega$ and $\Omega_{1/3} = \varnothing$. Lemma 5.1 established the Carleman estimate for the Laplace operator. Although such estimates are well known [13, 16], we still need to prove this lemma, because we use a non-standard CWF and also because when integrating the pointwise Carleman estimate over Ω, we should take into account that only one, rather than conventional two, zero boundary condition (5.1) is given at both Γ_2 and Γ_3. These were not done before.

Lemma 5.1. *Fix a number $\nu := \nu_0(\Omega) > 2$. Consider functions $u \in H^3(\Omega)$ such that (see (2.10a-c))*

$$u\mid_{\Gamma_1} = u_z\mid_{\Gamma_1} = u_x\mid_{\Gamma_2} = u_x\mid_{\Gamma_3} = 0. \tag{5.1}$$

Then there exists a constant $C = C(\Omega) > 0$ such that for any $\lambda > 2$ the following Carleman estimate is valid for all these functions

$$\begin{aligned}\int\limits_\Omega (\Delta u)^2 K^2 dxdz &\geq \frac{C}{\lambda}\int\limits_\Omega \left(u_{xx}^2 + u_{zz}^2 + u_{xz}^2\right) K^2 dxdz + C\lambda \int\limits_\Omega \left[(\nabla u)^2 + \lambda^2 u^2\right] K^2 dxdz \\ &\quad -C\lambda^3 \|u\|^2_{H^3(\Omega)} \exp\left[2\lambda\left(\frac{4}{3}\right)^{\nu_0}\right].\end{aligned}$$

Proof. It is convenient to assume initially that $\nu > 2$ is an arbitrary number. We have

$$\begin{aligned}(\Delta u)^2 K^2 &= \left(u_{xx}^2 + u_{zz}^2 + 2u_{xx}u_{zz}\right) K^2 = \\ &\quad \left(u_{xx}^2 + u_{zz}^2\right) K^2 + \partial_x\left(2u_x u_{zz} K^2\right) - 2u_x u_{zzx} K^2 + 4\lambda\nu\rho^{-\nu-1} u_x u_{zz} K^2 \\ &= \left(u_{xx}^2 + u_{zz}^2 + 2u_{xz}^2\right) K^2 + \partial_x\left(2u_x u_{zz} K^2\right) + \partial_z\left(-2u_x u_{xz} K^2\right) \\ &\quad +4\lambda\nu\rho^{-\nu-1}\left(u_x u_{zz} - u_x u_{zx}\right) K^2.\end{aligned}$$

Since

$$4\lambda\nu\rho^{-\nu-1}\left(u_x u_{zz} - u_x u_{xz}\right) K^2 \geq -\frac{1}{2}\left(u_{zz}^2 + u_{xz}^2\right) K^2 - 8\lambda^2\nu^2\rho^{-2\nu-2} u_x^2 K^2,$$

then we obtain that

$$\begin{aligned}(\Delta u)^2 K^2 &\geq \frac{1}{2}\left(u_{xx}^2 + u_{zz}^2 + u_{xz}^2\right) K^2 - 8\lambda^2\nu^2\rho^{-2\nu-2} u_x^2 K^2 \\ &\quad +\partial_x\left(2u_x u_{zz} K^2\right) + \partial_z\left(-2u_x u_{xz} K^2\right).\end{aligned} \tag{5.2}$$

Consider a new function $v = u \cdot K$. Substituting $u = v \cdot K^{-1}$, we obtain

$$\begin{aligned}(\Delta u)^2 \rho^{\nu+1} K^2 &= (y_1 + y_2 + y_3)^2 \rho^{\nu+1} \geq 2y_2(y_1 + y_3)\rho^{\nu+1}, \\ y_1 &= \Delta v,\ y_2 = 2\lambda\nu\rho^{-\nu-1} v_z,\ y_3 = (\lambda\nu)^2\rho^{-2\nu-2}\left(1 - \frac{\nu+1}{\lambda\nu}\rho^\nu\right) v.\end{aligned} \tag{5.3}$$

We have

$$2y_1 y_2 \rho^{\nu+1} = \partial_x\left(4\lambda\nu v_z v_x\right) + \partial_z\left[2\lambda\nu\left(v_z^2 - v_x^2\right)\right]. \tag{5.4}$$

Next, by (6.3)

$$\begin{aligned}2y_2 y_3 \rho^{\nu+1} &= 4(\lambda\nu)^3\left(\rho^{-2\nu-2} - \frac{\nu+1}{\lambda\nu}\rho^{-\nu-2}\right) v_z v \\ &= \partial_z\left[2(\lambda\nu)^3\left(\rho^{-2\nu-2} - \frac{\nu+1}{\lambda\nu}\rho^{-\nu-2}\right) v^2\right] \\ &\quad +4(\lambda\nu)^3(\nu+1)\rho^{-2\nu-3}\left(1 - \frac{\nu+2}{2\lambda\nu}\rho^\nu\right) v^2 \\ &\geq 2\lambda^3\nu^4\rho^{-2\nu-3} v^2 + \partial_z\left[2(\lambda\nu)^3\left(\rho^{-2\nu-2} - \frac{\nu+1}{\lambda\nu}\rho^{-\nu-2}\right) v^2\right].\end{aligned} \tag{5.5}$$

Summing up (5.4) and (5.5), using the backwards substitution $u = v \cdot K$ and using (5.3), we obtain

$$(\Delta u)^2 \rho^{\nu+1} K^2 \geq 2\lambda^3 \nu^4 \rho^{-2\nu-3} u^2 K^2 + \partial_x U_1 + \partial_z U_2, \tag{5.6}$$

where the following estimates are valid for functions U_1 and U_2

$$\begin{aligned} |U_1| &\leq C\lambda\nu \left|u_x\right| \left(\left|u_z\right| + \lambda\nu\rho^{-\nu-1}\left|u\right|\right) K^2, \\ |U_2| &\leq C\lambda\nu \left(\left|\nabla u\right|^2 + \lambda^2\nu^2\rho^{-2\nu-2}u^2\right) K^2. \end{aligned} \tag{5.7}$$

Since we do not have the term $\lambda \left(\nabla u\right)^2 K^2$ in the right hand side of (5.6),we continue as follows:

$$\begin{aligned} -\lambda\nu u \cdot \Delta u K^2 &= \partial_x \left(-\lambda\nu u u_x K^2\right) + \partial_z \left(-\lambda\nu u u_z K^2\right) + \lambda\nu \left(\nabla u\right)^2 K^2 - 2\lambda^2\nu^2\rho^{-\nu-1} u_z u K^2 \\ &= \lambda\nu \left(\nabla u\right)^2 K^2 - 2\lambda^3\nu^3\rho^{-2\nu-2}u^2K^2 + \partial_x U_3 + \partial_z U_4, \end{aligned}$$

Hence,

$$\begin{aligned} -\lambda\nu u \Delta u K^2 &= \lambda\nu \left(\nabla u\right)^2 K^2 - 2\lambda^3\nu^3\rho^{-2\nu-2}u^2K^2 + \partial_x U_3 + \partial_z U_4, \\ U_3 &= -\lambda\nu u u_x K^2, |U_4| \leq C\left(\lambda\nu u_z^2 + \lambda^2\nu^2\rho^{-\nu-1}u^2\right) K^2. \end{aligned} \tag{5.8}$$

Add (6.8) to (6.6) and take into account (6.7) as well as the fact that $2\lambda^3\nu^4\rho^{-2\nu-3} > 4\lambda^3\nu^3\rho^{-2\nu-2}$ for $\nu > 2$. Likewise, by the Cauchy inequality $-\lambda\nu u \cdot \Delta u K^2 \leq \lambda^2\nu^2\rho^{-\nu-1}u^2K^2/2 + (\Delta u)^2\rho^{\nu+1}K^2/2$. Fix the number $\nu := \nu_0 > 2$. Then we can incorporate ν_0 in C and also we can regard that $\rho^{\nu_0+1} < C$, since $\rho^{\nu_0+1} < 1$. Hence, we obtain

$$\begin{aligned} (\Delta u)^2 K^2 &\geq C\lambda\left[\left(\nabla u\right)^2 + \lambda^2 u^2\right] K^2 + \partial_x U_5 + \partial_z U_6, \\ |U_5| &\leq C\lambda \left|u_x\right| \left(\left|u_z\right| + \lambda\left|u\right|\right) K^2, \ \ |U_6| \leq C\lambda\left[\left|\nabla u\right|^2 + \lambda^2 u^2\right] K^2. \end{aligned} \tag{5.9}$$

Now we set in (5.2) $\nu := \nu_0$, divide it by λd with a positive constant $d = d\left(\nu_0\right)$ such that $4\lambda\nu_0^2\rho^{-2\nu_0-2}/d \leq C/2$ and next add it to (5.9). Then we can choose a constant obtain the following pointwise Carleman estimate for the Laplace operator in the domain Ω

$$\begin{aligned} (\Delta u)^2 K^2 &\geq \frac{C}{\lambda}\left(u_{xx}^2 + u_{zz}^2 + u_{xz}^2\right) K^2 + C\lambda\left[\left(\nabla u\right)^2 + \lambda^2 u^2\right] K^2 + \partial_x U_7 + \partial_z U_8, \\ |U_7| &\leq C\lambda \left|u_x\right| \left(\left|u_{zz}\right| + \left|u_z\right| + \lambda\left|u\right|\right) K^2, \ \ |U_8| \leq C\lambda\left[\left|u_{xz}\right|^2 + \left|\nabla u\right|^2 + \lambda^2 u^2\right] K^2. \end{aligned} \tag{5.10}$$

We now integrate (5.10) over the rectangle Ω using the Gauss-Ostrogradsky formula. It is important that because of (5.1) and the estimate for $|U_7|$, resulting boundary integrals over Γ_1, Γ_2 and Γ_3 will be zero. Finally, to obtain the estimate of this lemma, we note that

$$K^2\left(\frac{1}{2}\right) = K^2\left(z\right)|_{\Gamma_4} = \min_{\overline{\Omega}} K^2\left(z\right) = \exp\left[2\lambda\left(\frac{4}{3}\right)^{\nu_0}\right].$$

Thus,

$$\int\limits_{\Gamma_4} \lambda\left[\left|u_{xz}\right|^2 + \left|\nabla u\right|^2 + \lambda^2 u^2\right] K^2 dx \leq C\lambda^3 \left\|u\right\|_{H^3(\Omega)}^2 \exp\left[2\lambda\left(\frac{4}{3}\right)^{\nu_0}\right]. \ \square$$

We now establish both existence and uniqueness of the minimizer of the functional (4.7).

Lemma 5.2. *Suppose that in (4.7)* $H_{n,k} \in L_2(\Omega)$ *and that there exists a function* $\Phi \in H^5(\Omega)$ *satisfying boundary conditions (4.6), except of maybe at* Γ_4. *Assume that in (4.4) both components* $a_{n,k}^{(j)}, j = 1, 2$ *of the vector function* $a_{n,k}$ *are such that* $a_{n,k}^{(j)} \in C\left(\overline{\Omega}\right)$ *and* $\left\|a_{n,k}^{(j)}\right\|_{C\left(\overline{\Omega}\right)} \leq 1$. *Then there exists unique minimizer* $u_\varepsilon \in H^5(\Omega)$ *of the functional (5.7). Furthermore,*

$$\|u_\varepsilon\|_{H^5(\Omega)} \leq \frac{C}{\sqrt{\alpha}} \left(\|H_{n,k}\|_{L_2(\Omega)} + \|\Phi\|_{H^5(\Omega)} \right).$$

Proof. We assume here that $\left\|a_{n,k}^{(j)}\right\|_{C\left(\overline{\Omega}\right)} \leq 1$ for the purpose of Theorem 6.1 only, since actually we can impose any *a priori* upper estimate on these numbers. Let u be a minimizer of $J_{n,k}^{\alpha}(u)$ satisfying boundary conditions (4.6). Denote $U = u - \Phi$. The function U satisfies boundary conditions (5.1). By the variational principle

$$(G_{n,k}U, G_{n,k}v) + \alpha [U, v] = (H_{n,k} - G_{n,k}\Phi, G_{n,k}v),$$

for all functions $v \in H^5(\Omega)$ satisfying boundary conditions (5.1). Here

$$G_{n,k}U := \Delta U - a_{n,k} \cdot \nabla U. \tag{5.11}$$

Here and below $(\cdot, \cdot)$ denotes the scalar product in $L_2(\Omega)$ and $[\cdot, \cdot]$ denotes the scalar product in $H^5(\Omega)$. The rest of the proof follows from the Riesz theorem. $\square$

In the course of the proof of Theorem 6.1 we will need

Lemma 5.3. *Consider an arbitrary function* $g \in H^5(\Omega)$. *Let the function* $u \in H^5(\Omega)$ *satisfies boundary conditions (5.1) as well as the variational equality*

$$(G_{n,k}u, G_{n,k}v) + \alpha [u, v] = (H_{n,k}, G_{n,k}v) + \alpha [g, v], \tag{5.12}$$

for all functions $v \in H^5(\Omega)$ *satisfying (5.1). Then*

$$\|u\|_{H^5(\Omega)} \leq \frac{\|H_{n,k}\|_{L_2(\Omega)}}{\sqrt{\alpha}} + \|g\|_{H^5(\Omega)}.$$

Proof. Set in (5.12) $v := u$ and use the Cauchy-Schwarz inequality. $\square$

Theorem 5.1. *Consider an arbitrary function* $g \in H^5(\Omega)$. *Let* $u \in H^5(\Omega)$ be the function satisfying (5.1) and (5.12). Let $\left\|a_{n,k}^{(j)}\right\|_{C\left(\overline{\Omega}\right)} \leq 1$, *where* $a_{n,k}^{(j)}, j = 1, 2$ *are two components of the vector function* $a_{n,k}$ *in (5.4). Choose an arbitrary number* $\overline{\varkappa}$ *such that* $\overline{\varkappa} \in (\varkappa, 1)$. *Consider the numbers* b_1, b_2,

$$b_1 = \frac{1}{2\left(1 + (1 - \overline{\varkappa}^{\nu_0})(3\overline{\varkappa})^{-\nu_0}\right)} < \frac{1}{2}, \; b_2 = \frac{1}{2} - b_1 > 0,$$

where ν_0 is the parameter of Lemma 5.1. Then there exists a sufficiently small number $\alpha_0 = \alpha_0(\nu_0, \varkappa, \overline{\varkappa}) \in (0,1)$ such that for all $\alpha \in (0, \alpha_0)$ the following estimate holds

$$\|u\|_{H^2(\Omega_\varkappa)} \leq C\frac{\|H_{n,k}\|_{L_2(\Omega)}}{\alpha^{b_1}} + \alpha^{b_2}\|g\|_{H^5(\Omega)}.$$

Proof. Setting (5.12) $v := u$ and using the Cauchy-Schwarz inequality, we obtain

$$\|G_{n,k}u\|^2_{L_2(\Omega)} \leq F^2 := \|H_{n,k}\|^2_{L_2(\Omega)} + \alpha\|g\|^2_{H^5(\Omega)}. \tag{5.13}$$

Note that $K^2(0) = \max_{\overline{\Omega}} K^2(z) = \exp(2\lambda \cdot 4^{\nu_0})$. Hence, $K^{-2}(0)\|K \cdot G_{n,k}u\|^2_{L_2(\Omega)} \leq F^2$. Clearly $(G_{n,k}u)^2 K^2 \geq (\Delta u)^2 K^2/2 - C(\nabla u)^2 K^2$. Hence,

$$\int\limits_\Omega (\Delta u)^2 K^2 dxdz \leq C\int\limits_\Omega (\nabla u)^2 K^2 dxdz + K^2(0)F^2. \tag{5.14}$$

Applying Lemma 5.1 to (5.14), choosing $\lambda > 1$ sufficiently large and observing that the term with $(\nabla u)^2$ in (5.14) will be absorbed for such λ, we obtain

$$\begin{aligned}
&\lambda K^2(0)F^2 + C\lambda^4\|u\|^2_{H^3(\Omega)}\exp\left[2\lambda\left(\frac{4}{3}\right)^{\nu_0}\right]\\
\geq\ & C\int\limits_\Omega \left(u^2_{xx} + u^2_{zz} + u^2_{xz} + |\nabla u|^2 + u^2\right)K^2 dxdz\\
\geq\ & C\int\limits_{\Omega_\varkappa} \left(u^2_{xx} + u^2_{zz} + u^2_{xz} + |\nabla u|^2 + u^2\right)K^2 dxdz\\
\geq\ & C\exp\left[2\lambda\left(\frac{4}{3\varkappa}\right)^{\nu_0}\right]\|u\|^2_{H^2(\Omega)}.
\end{aligned}$$

Comparing the first line with the last in this sequence of inequalities, dividing by the exponential term in the last line, taking $\lambda \geq \lambda_0(C, \varkappa, \overline{\varkappa}) > 1$ sufficiently large and noting that for such λ

$$\lambda^4\exp\left[-2\lambda\left(\frac{4}{3\varkappa}\right)^{\nu_0}\right] < \exp\left[-2\lambda\left(\frac{4}{3\overline{\varkappa}}\right)^{\nu_0}\right],$$

we obtain a stronger estimate,

$$\|u\|^2_{H^2(\Omega_\varkappa)} \leq CK^2(0)F^2 + C\|u\|^2_{H^3(\Omega)}\exp\left[-2\lambda\left(\frac{4}{3\overline{\varkappa}}\right)^{\nu_0}(1-\overline{\varkappa}^{\nu_0})\right] \tag{5.15}$$

Applying Lemma 5.3 to the second term in the right hand side of (5.15), we obtain

$$\|u\|^2_{H^2(\Omega_\varkappa)} \leq CF^2\left\{\exp(2\lambda\cdot 4^{\nu_0}) + \alpha^{-1}\exp\left[-2\lambda\left(\frac{4}{3\overline{\varkappa}}\right)^{\nu_0}(1-\overline{\varkappa}^{\nu_0})\right]\right\}. \tag{5.16}$$

Since $\alpha \in (0, \alpha_0)$ and α_0 is sufficiently small, we can choose sufficiently large $\lambda = \lambda(\alpha)$ such that

$$\exp(2\lambda \cdot 4^{\nu_0}) = \alpha^{-1} \exp\left[-2\lambda \left(\frac{4}{3\overline{\varkappa}}\right)^{\nu_0} (1 - \overline{\varkappa}^{\nu_0})\right]. \tag{5.17}$$

We obtain from (5.17) that $2\lambda \cdot 4^{\nu_0} = \ln \alpha^{-2b_1}$. Hence, (5.13) and (5.15)-(5.17) imply the validity of this theorem. $\square$

6 Global Convergence Theorem

We follow the concept of Tikhonov for ill-posed problems [18]. By this concept, one should assume that there exists an "ideal" exact solution of an ill-posed problem with the "ideal" exact data. Next, one should prove that the regularized solution is close to the exact one.

6.1 Exact solution

First, we need to introduce the definition of the exact solution. We assume that there exists a coefficient $c^*(\mathbf{x})$ satisfying conditions (2.3), (2.4), and this function is the unique exact solution of our Inverse Problem with the exact data $\varphi_0^*(x,s), \varphi_1^*(x,s)$ in (2.11), where $\varphi_0^*(x,s) = w^*(x,0,s)$, $\varphi_1^*(x,s) = w_z^*(x,0,s)$, $\forall s \in [\underline{s}, \overline{s}]$. Here the function $w^*(\mathbf{x},s) \in C^{5+\gamma}(\mathbb{R}^2 \setminus \{|\mathbf{x} - \mathbf{x}_0| < \varepsilon\}) \times C^2([\underline{s}, \overline{s}])$, $\forall \varepsilon > 0$, $\forall \gamma \in (0,1), \forall s \geq \underline{s}$ is the solution of the forward problem (2.6), (2.7) with $c(\mathbf{x}) := c^*(\mathbf{x})$. Let

$$v^*(\mathbf{x},s) = s^{-2} \ln[w^*(\mathbf{x},s)], \; q^*(\mathbf{x},s) = \partial_s v^*(\mathbf{x},s), \; V^*(\mathbf{x}) = v^*(\mathbf{x},\overline{s}).$$

Hence, $q^*(\mathbf{x},s) \in C^{5+\gamma}(\Omega) \times C^1[\underline{s}, \overline{s}]$. By (3.1)

$$c^*(\mathbf{x}) = \Delta v^*(\mathbf{x},s) + s^2 |\nabla v^*(\mathbf{x},s)|^2, \forall s \in [\underline{s}, \overline{s}]. \tag{6.1}$$

The function q^* satisfies equation (3.7) where V is replaced with V^*. Boundary conditions for q^* are the same as ones (3.8), (3.9), where functions $\psi_0(x,s), \psi_1(x,s)$ are replaced with the exact boundary conditions $\psi_0^*(x,s), \psi_1^*(x,s)$ for $s \in [\underline{s}, \overline{s}]$,

$$q^*|_{\Gamma_1} = \psi_0^*(x,s), q_z^*|_{\Gamma_1} = \psi_1^*(x,s), \; \partial_{\nu_i} q^* \,|_{\Gamma_i} = s^{-2}, \; i = 2,3,4. \tag{6.2}$$

We call the function $q^*(\mathbf{x},s)$ *the exact solution* of the problem (3.7)-(3.9) with the exact boundary conditions (6.2). For $n \geq 1$ let q_n^*, $\overline{\psi}_{0,n}^*$ and $\overline{\psi}_{1,n}^*$ be averages of functions q^*, ψ_0^* and ψ_1^* over the interval (s_n, s_{n-1}). Hence, it is natural to assume that

$$q_0^* \equiv 0, \max_{1 \leq n \leq N} \|q_n^*\|_{H^5(\Omega)} \leq C^*, C^* = const. > 1, \tag{6.3}$$

$$\left\|\overline{\psi}_{0,n}^* - \overline{\psi}_{0,n}\right\|_{H^2(\Gamma_1)} + \left\|\overline{\psi}_{1,n}^* - \overline{\psi}_{1,n}\right\|_{H^1(\Gamma_1)} \leq C^*(\sigma + h), \tag{6.4}$$

$$\max_{s \in [s_n, s_{n-1}]} \|q_n^* - q^*\|_{H^5(\Omega)} \leq C^* h \tag{6.5}$$

Here the constant $C^* = C^*\left(\|q^*\|_{H^5(\Omega)\times C^1[\underline{s},\overline{s}]}\right)$ depends only on the $C^5\left(\overline{\Omega}\right)\times C^1\left[\underline{s},\overline{s}\right]$ norm of the function $q^*(\mathbf{x},s)$ and $\sigma>0$ is a small parameter characterizing the level of the error in the data $\psi_0(x,s),\psi_1(x,s)$. We use the $H^5(\Omega)$ norm because of the quasi-reversibility, see (4.7). The step size $h=s_{n-1}-s_n$ can also be considered as a part of the error in the data. In addition, because of (6.2)

$$q_n^*|_{\Gamma_1}=\overline{\psi}_{0,n}^*(x),\partial_z q_n^*|_{\Gamma_1}=\overline{\psi}_{1,n}^*(x),\partial_\nu q_n^*|_{\Gamma_i}=\left(s_n s_{n-1}\right)^{-1},i=2,3,4. \tag{6.6}$$

The function q_n^* satisfies the following analogue of equation (3.11)

$$\begin{aligned}&\Delta q_n^*-A_{1,n}\left(h\sum_{i=1}^{n-1}\nabla q_i^*(x)-\nabla V^*\right)\cdot\nabla q_n^*=-A_{2,n}h^2\left(\sum_{i=1}^{n-1}\nabla q_i^*(x)\right)^2\\&+2A_{2,n}\nabla V^*\cdot\left(h\sum_{i=1}^{n-1}\nabla q_i^*(x)\right)-A_{2,n}\left(\nabla V^*\right)^2+F_n(x,h,\mu).\end{aligned} \tag{6.7}$$

Since we have dropped the nonlinear term $B_n\left(\nabla q_n\right)^2$ in (4.1) (Remark 3.2), we incorporate this term in the error function $F_n(x,h,\mu)\in L_2(\Omega)$ in (6.7). So, it is reasonably to assume that

$$\max_{\mu h\geq 1}\|F_n(\mathbf{x},h,\xi,\mu)\|_{L_2(\Omega)}\leq C^*\left(h+\mu^{-1}\right). \tag{6.8}$$

6.2 Global convergence theorem

Assume that

$$\overline{s}>1,\ \mu h\geq 1. \tag{6.9}$$

Then [1]

$$\max_{1\leq n\leq N}\left\{|A_{1,n}|+|A_{2,n}|\right\}\leq 8\overline{s}^2. \tag{6.10}$$

We assume for brevity that

$$\overline{\psi}_{0,n}^*=\overline{\psi}_{0,n},\overline{\psi}_{1,n}^*=\overline{\psi}_{1,n}. \tag{6.11}$$

The proof of Theorem 6.1 for the more general case (6.4) can easily be extended along the same lines, although it would take more space. Still, we keep the parameter σ of (6.4) as a part of the error in the data and incorporate it in the function F_n. Thus, we obtain instead of (6.8)

$$\max_{\mu h\geq 1}\|F_n(\mathbf{x},h,\xi,\mu)\|_{L_2(\Omega)}\leq C^*\left(h+\mu^{-1}+\sigma\right). \tag{6.12}$$

We also recall that by the embedding theorem $H^5(\Omega)\subset C^3\left(\overline{\Omega}\right)$ and

$$\|f\|_{C^3\left(\overline{\Omega}\right)}\leq C\|f\|_{H^5(\Omega)},\forall f\in H^5(\Omega). \tag{6.13}$$

Theorem 6.1. *Let the exact coefficient $c^*(\mathbf{x})$ satisfy conditions (2.3), (2.4). Suppose that conditions (6.2)-(6.9), (6.11) and (6.12) are satisfied. Assume that for each $n\in[1,N]$*

there exists a function $\Phi_n \in H^5(\Omega)$ *satisfying boundary conditions (4.6), except of maybe at* Γ_4. *For any function* $c \in C^\gamma(\mathbb{R}^2)$ *such that* $c(\mathbf{x}) \geq 1/2$, $c(\mathbf{x}) = 1$ *in* $\mathbb{R}^2 \setminus \Omega$ *consider the solution* $w_c(\mathbf{x}, \overline{s}) \in C^{2+\gamma}(\mathbb{R}^2 \setminus \{|\mathbf{x} - \mathbf{x}_0| < \theta\}), \forall \theta > 0$ *of the problem (2.6), (2.7). Let* $V_c(\mathbf{x}) = \overline{s}^{-2} \ln w_c(\mathbf{x}, \overline{s}) \in C^{2+\gamma}(\mathbb{R}^2 \setminus \{|\mathbf{x} - \mathbf{x}_0| < \theta\}), \theta > 0$ *be the corresponding tail function and* $V_{1,1}(\mathbf{x}, \overline{s}) \in C^2\left(\overline{\Omega}\right)$ *be the initial tail function. Suppose that the cut-off pseudo frequency* $\overline{s}$ *is so large that the following estimates hold*

$$\|V^*\|_{C^1\left(\overline{\Omega}\right)} \leq \frac{\xi}{2}, \|V_{1,1}\|_{C^1\left(\overline{\Omega}\right)} \leq \frac{\xi}{2}, \|V_c\|_{C^1\left(\overline{\Omega}\right)} \leq \frac{\xi}{2}, \tag{6.14}$$

for any such function $c(\mathbf{x})$. *Here* $\xi \in (0,1)$ *is a sufficiently small number. Introduce the parameter* $\beta := \overline{s} - \underline{s}$, *which is the total length of the s-interval covered in our algorithm. Let* α_0 *be so small that it satisfies the corresponding condition of Theorem 5.1. Let* $\alpha \in (0, \alpha_0)$ *be the regularization parameter of the QRM. Assume that numbers* h, σ, ξ, β, *are so small that*

$$h + \mu^{-1} + \sigma + \xi \leq \beta, \tag{6.15}$$

$$\beta \leq \frac{\sqrt{\alpha}}{136\overline{s}^2 (C^*)^2 C_1}, \tag{6.16}$$

where the number b_2 *was introduced in Theorem 5.1 and the constant* C_1 *depends only on the domain* Ω. *We assume without loss of generality that* $C_1 \in (1, C^*)$. *Then the following estimates hold for all* $\alpha \in (0, \alpha_0)$ *and all* $n \in [1, N]$

$$\|q_n\|_{H^5(\Omega)} \leq 3C^*, \tag{6.17}$$

$$\|q_n - q_n^*\|_{H^2(\Omega_\varkappa)} \leq 2C^* \alpha^{b_2}, \tag{6.18}$$

$$\|c_n - c^*\|_{C^1\left(\overline{\Omega}_\varkappa\right)} \leq 2C^* \alpha^{b_2}, c_n \geq \frac{1}{2} \text{ in } \Omega_\varkappa. \tag{6.19}$$

Remarks 6.1.

1. Because of the term $\overline{s}^{-2}$ in inequalities (6.16), there is a discrepancy between these inequalities and (3.6). This discrepancy was discussed in detail in subsection 3.3 of [12] and in subsection 6.3 of [2], also see Introduction above. A new mathematical model proposed in these references allows the parameter ξ in (6.14) to become infinitely small independently on the truncation pseudo frequency $\overline{s}$, also see discussion in the Introduction section above. We point out that this mathematical model was verified on experimental data. Indeed, actually the derivatives $\partial_{\overline{s}} V_{n,k}$ instead of functions $V_{n,k}$ were used in the numerical implementation of [12], and this implementation was done prior experimental data were actually measured, see subsections 7.1 and 7.2 of [12]. It follows from (3.6) that one should expect that $\|\partial_{\overline{s}} V_{n,k}\|_{C^2\left(\overline{\Omega}\right)} << \|V_{n,k}\|_{C^2\left(\overline{\Omega}\right)} = O(1/\overline{s}), \overline{s} \to \infty$. Finally, we believe that, as in any applied problem, the independent verification on *blind* experimental data in [12] represents a valuable justification of this new mathematical model.

2. In our definition "global convergence" means that, given the above new mathematical model, there is a rigorous guarantee that a good approximation for the exact solution can

be obtained, regardless on the availability of a good first guess about this solution. Furthermore, such a global convergence analysis should be confirmed by numerical experiments. So, Theorem 6.1, complemented by our numerical results below, satisfies these requirements.

3. The assumption of the smallness of the parameter $\beta = \overline{s} - \underline{s}$ is a natural one because equations (4.1) are actually generated by equation (3.7), which contains the nonlinearity in Volterra-like integrals. It is well known from the standard Ordinary Differential Equations course that solutions of nonlinear integral Volterra-like equations might have singularities on large intervals.

Proof of Theorem 6.1. Denote $\widetilde{q}_{n,k} = q_{n,k} - q_n^*, \widetilde{V}_{n,k} = V_{n,k} - V^*$. By (6.14)

$$\left\| \widetilde{V}_{n,k} \right\|_{C^1(\overline{\Omega})} \leq \xi. \tag{6.20}$$

This proof basically consists in estimating norms $\|\widetilde{q}_{n,k}\|_{H^i(\Omega_\varkappa)}$ from the above. Compared with proofs in [1, 2], the main difficulty here is that we have to analyze integral identities resulting from the QRM, instead of pointwise equations of [1, 2]. Hence, we use results of Theorem 5.1 here instead of the Schauder theorem of [1]. Recall that $(\cdot,\cdot)$ denotes the scalar product in $L_2(\Omega)$ and $[\cdot,\cdot]$ denotes the scalar product in $H^5(\Omega)$.

Since by (3.12) and (6.5) $q_0 \equiv q_0^* \equiv 0$, then (6.17) and (6.18) are true for $n = 0$. Assume that they are true for functions q_j with $j \leq n-1, n \geq 1$. Below we will prove them for $j := n$. Denote $Q_n^* = q_n^* - \Phi_n, Q_{n,k} = q_{n,k} - \Phi_n$. Below in this proof $v \in H^5(\Omega_n)$ is an arbitrary function satisfying (5.1). Let $G_{n,k}^*$ be the operator in the left hand side of (6.7). Let $H_{n,k}^*$ be the right hand side of (6.7). Substituting in (6.7) $q_n^* := Q_n^* + \Phi_n$, multiplying both sides by the function $G_{n,k}v$, integrating over Ω and then adding to both sides $\alpha[q_n^*, v]$, we obtain

$$\left(G_{n,k}^* Q_n^*, G_{n,k}v\right) + \alpha[Q_n^* + \Phi_n, v] = \left(H_{n,k}^* - G_{n,k}\Phi_n, G_{n,k}v\right) + \alpha[q_n^*, v]. \tag{6.21}$$

It follows from the proof of Lemma 5.2 that

$$(G_{n,k}Q_{n,k}, G_{n,k}v) + \alpha[Q_{n,k} + \Phi_n, v] = (H_{n,k} - G_{n,k}\Phi_n, G_{n,k}v). \tag{6.22}$$

Subtracting (6.21) from (6.22), we obtain

$$\left(G_{n,k}Q_{n,k} - G_{n,k}^* Q_n^*, G_{n,k}v\right) + \alpha[\widetilde{q}_{n,k}, v] = \left(H_{n,k} - H_{n,k}^*, G_{n,k}v\right) - \alpha[q_n^*, v], \tag{6.23}$$

Elementary calculations show that (6.23) is equivalent with

$$(G_{n,k}\widetilde{q}_{n,k}, G_{n,k}v) + \alpha[\widetilde{q}_{n,k}, v] = (P_{n.k}, G_{n,k}v) - \alpha[q_n^*, v]. \tag{6.24}$$

In addition, it follows from (6.11) that

$$\widetilde{q}_{n,k}\mid_{\Gamma_1} = \partial_z \widetilde{q}_{n,k}\mid_{\Gamma_1} = \partial_x \widetilde{q}_{n,k}\mid_{\Gamma_2} = \partial_x \widetilde{q}_{n,k}\mid_{\Gamma_3} = 0. \tag{6.25}$$

The function $P_{n.k}$ in (6.24) is

$$\begin{aligned} P_{n.k}(x) &= -A_{1,n}\left(h\sum_{j=1}^{n-1}\nabla\widetilde{q}_j - \widetilde{V}_{n,k}\right)\nabla q_n^* \\ &\quad -A_{2,n}\left(h\sum_{j=1}^{n-1}\nabla\widetilde{q}_j\right)\left(h\sum_{j=1}^{n-1}\left(\nabla q_j + \nabla q_j^*\right) - 2\nabla V_{n,k}\right) \\ &\quad +A_{2,n}\nabla\widetilde{V}_{n,k}\cdot\left(2h\sum_{j=1}^{n-1}\nabla q_j^* - \left(\nabla V_{n,k} + \nabla V^*\right)\right) - F_n. \end{aligned} \tag{6.26}$$

It follows from (6.14)-(6.16) as well as from (6.17) for $q_j, j \leq n-1$ that components of the vector function $a_{n,k}$ in the operator $G_{n,k}$ satisfy the corresponding condition of Theorem 5.1, $\left\|a_{n,k}^{(i)}\right\|_{C(\overline{\Omega})} \leq 1, i = 1, 2$. Hence, Lemma 5.3 and Theorem 5.1, (6.3), (6.24) and (6.25) imply that

$$\|\widetilde{q}_{n,k}\|_{H^5(\Omega)} \leq \frac{\|P_{n,k}\|_{L_2(\Omega)}}{\sqrt{\alpha}} + C^*, \tag{6.27}$$

$$\|\widetilde{q}_{n,k}\|_{H^2(\Omega_\varkappa)} \leq C_1\frac{\|P_{n,k}\|_{L_2(\Omega)}}{\alpha^{b_1}} + \alpha^{b_2}C^*. \tag{6.28}$$

It follows from (6.27) and (6.28) that we now need to estimate the norm $\|P_{n,k}\|_{L_2(\Omega)}$ from the above. First, using (6.3), (6.10), (6.14), (6.15) as well as (6.17) and (6.18) for $q_j, j \leq n-1$, we obtain

$$\left\|-A_{1,n}\left(h\sum_{j=1}^{n-1}\nabla\widetilde{q}_j - V_{n,k}\right)\nabla q_n^*\right\|_{L_2(\Omega)} \leq 24\overline{s}^2\left(C^*\right)^2 C_1\beta. \tag{6.29}$$

Similarly we obtain

$$\left\|A_{2,n}\left(h\sum_{j=1}^{n-1}\nabla\widetilde{q}_j\right)\left(h\sum_{j=1}^{n-1}\left(\nabla q_j + \nabla q_j^*\right) - 2\nabla V_{n,k}\right)\right\|_{L_2(\Omega)} \leq 80\overline{s}^2\left(C^*\right)^2 C_1\beta. \tag{6.30}$$

Likewise,

$$\left\|A_{2,n}\nabla\widetilde{V}_{n,k}\cdot\left(2h\sum_{j=1}^{n-1}\nabla q_j^* - \left(\nabla V_{n,k} + \nabla V^*\right)\right) - F_n\right\|_{L_2(\Omega)} \leq 32\overline{s}^2 C^* C_1\beta. \tag{6.31}$$

Summing up (6.29)-(6.31), we obtain $\|P_{n,k}\|_{L_2(\Omega)} \leq \left[136\overline{s}^2\left(C^*\right)^2 C_1\right]\beta$. Hence, (6.16) implies that

$$\|P_{n,k}\|_{L_2(\Omega)} \leq \sqrt{\alpha}. \tag{6.32}$$

Hence, using (6.27), (6.28) and (6.32), we obtain

$$\|\widetilde{q}_{n,k}\|_{H^5(\Omega)} \leq 2C^*, \|\widetilde{q}_{n,k}\|_{H^2(\Omega_\varkappa)} \leq 2C^*\alpha^{b_2}. \tag{6.33}$$

The second inequality (6.33) proves (6.18). To prove (6.17), we use the first inequality (6.33) in $\|q_{n,k}\|_{H^5(\Omega)} \leq \|\widetilde{q}_{n,k}\|_{H^5(\Omega)} + \|q_n^*\|_{H^5(\Omega)} \leq 3C^*$. As soon as (6.17) and (6.18) are established, the proof of the first inequality (6.19) is straightforward. To do so, one needs to subtract (6.1) from (4.3) and then use (6.13), (6.17), (6.18), (4.2) and (6.5) in a straightforward manner. The second inequality (6.19) follows from (2.3) and the smallness condition imposed on the number α_0. $\square$

7 A Simplified Mathematical Model of Imaging of Antipersonnel Plastics Land Mines

The first main simplification of our model is that we consider the 2-D instead of the 3-D case. Second, we ignore the air/ground interface, assuming that the governing PDE is valid on the entire 2-D plane. The third simplification is that we consider a plane wave instead of the point source in (2.1). This is because our current computer code is designed only for the plane wave. As it is always the case of sophisticated computer codes, it takes quite an effort to re-design it for the case of a point source and this work is currently underway. The point source was considered above only for the convenience of analytical derivations due to Lemma 2.1.

Let the ground be $\{\mathbf{x} = (x, z) : z > 0\} \subset \mathbb{R}^2$. Suppose that a polarized electric field is generated by a plane wave, which is initialized at the point $(0, z^0), z^0 < 0$ at the moment of time $t = 0$. The following hyperbolic equation can be derived from Maxwell equations [7]

$$\begin{aligned} \varepsilon_r(\mathbf{x})u_{tt} &= \Delta u,\ (\mathbf{x}, t) \in \mathbb{R}^2 \times (0, \infty), & (7.1)\\ u(\mathbf{x}, 0) &= 0,\ u_t(\mathbf{x}, 0) = \delta\left(z - z^0\right), & (7.2) \end{aligned}$$

where the function $u(\mathbf{x}, t)$ is a component of the electric field. Recall that $\varepsilon_r(\mathbf{x})$ is the spatially distributed dielectric constant, see the beginning of section 2. We assume that the function $\varepsilon_r(\mathbf{x})$ satisfies the same conditions (2.3), (2.4) as the function $c(\mathbf{x})$. The Laplace transform (2.5) leads to the following analog of the problem (2.6), (2.7)

$$\begin{aligned} \Delta w - s^2\varepsilon_r(\mathbf{x})w &= -\delta\left(z - z^0\right), \forall s \geq \underline{s}, & (7.3)\\ \lim_{|\mathbf{x}|\to\infty} (w - w_0)(\mathbf{x}, s) &= 0, \forall s \geq \underline{s}, & (7.4) \end{aligned}$$

where $w_0(z, s) = \exp(-s|z - z_0|)/(2s)$ is such a solution of equation (7.3) for the case $\varepsilon_r(\mathbf{x}) \equiv 1$ that $\lim_{|z|\to\infty} w_0(z, s) = 0$.

It is well known that the maximal depth of an antipersonnel land mine does not exceed about 10 cm=0.1 m. So, we model these mines as small squares with the 0.1 m length of sides, and their centers should be at the maximal depth of 0.1 m. We set $\Omega =$

$\{\mathbf{x} = (x, z) \in (-0.3m, 0.3m) \times (0m, 0.6m)\}$. Consider dimensionless variables $\mathbf{x}' = \mathbf{x}/0.1, z^{0\prime} = z^0/0.1$. For brevity we keep the same notations both for these variables and the new domain Ω,

$$\Omega = (-3, 3) \times (0, 6). \tag{7.5}$$

We now use the values of the dielectric constant given at http://www.clippercontrols.com. Hence, $\varepsilon_r = 5$ in the dry sand and $\varepsilon_r = 22$ in the trinitrotoluene (TNT). We also take $\varepsilon_r = 2.5$ in a piece of wood submersed in the ground. Hence,

$$\frac{\varepsilon_r\,(\text{TNT})}{\varepsilon_r\,(\text{dry sand})} = \frac{22}{5} \approx 4.$$

Since the dry sand should be considered as a background outside of our domain of interest Ω, we introduce parameters $\varepsilon_r' = \varepsilon_r/5, s' = s \cdot 0.1 \cdot \sqrt{5}$, and again do not change notations. Then relations (7.3) and (7.4) are valid. Hence, we now can assume that the following values of this scaled dielectric constant

$$\varepsilon_r\,(\text{dry sand}) = 1, \varepsilon_r\,(\text{TNT}) = 4, \varepsilon_r\,(\text{piece of wood}) = 0.5. \tag{7.6}$$

In addition, centers of small squares modeling our targets should be in the rectangle

$$\{\mathbf{x} = (x, z) \in [-2.5, 2.5] \times [0.5, 1.0]\}. \tag{7.7}$$

The side of each of our small square should be 1, i.e. 10 cm. The interval $[0.5, 1.0]$ in (7.7) corresponds to depths of centers between 5 cm and 10 cm and the interval $[-2.5, 2.5]$ means that any such square is fully inside of Ω. Hence, an accurate image of the location of that small square as well as of the value of the coefficient $\varepsilon_r(\mathbf{x})$ both inside and outside of it would provide a useful information about the possible presence of a land mine and also might help to differentiate between mines and non-mines.

8 Numerical Studies

In this paper, we work only with the computationally simulated data. The data are generated by solving numerically equation (7.3) in the rectangle $R = [-4, 4] \times [-2, 8]$. By (7.5) $\Omega \subset R$. To avoid the singularity in $\delta(z - z^0)$, we actually solve in R the equation for the function $\widetilde{w} = w - w_0$ with zero Dirichlet boundary condition for this function, see (7.4). We solve the resulting Dirichlet boundary value problem via the FDM with the uniform mesh size $h_f = 0.0675$.

It is quite often the case in numerical studies, one should slightly modify the numerical scheme given by the theory, and so we did the same. Indeed, it is well known in computations that numerical results are usually more optimistic than analytical ones. We have modified our above algorithm via considering the function $\widetilde{v} = s^{-2} \cdot \ln(w/w_0)$. In other words, we have divided our solution w of the problem (7.3), (7.4) by the initializing plane wave w_0. This has resulted in an insignificant modification of equations (4.1). We have observed in our

computations that the function w/w_0 at the measurement part $\Gamma_1 \subset \partial\Omega$ is poorly sensitive to the presence of abnormalities, as long as $s > 1.2$, see Figure 1-b). Hence, one should expect that the modified tail function for the function $\widetilde{v}$ should be small for $s > 1.2$, which is exactly what is required by the above theory. For this reason, we have chosen the truncation pseudo frequency $\overline{s} = 1.2$ and the initial tail function $V_{1,1} \equiv 0$.

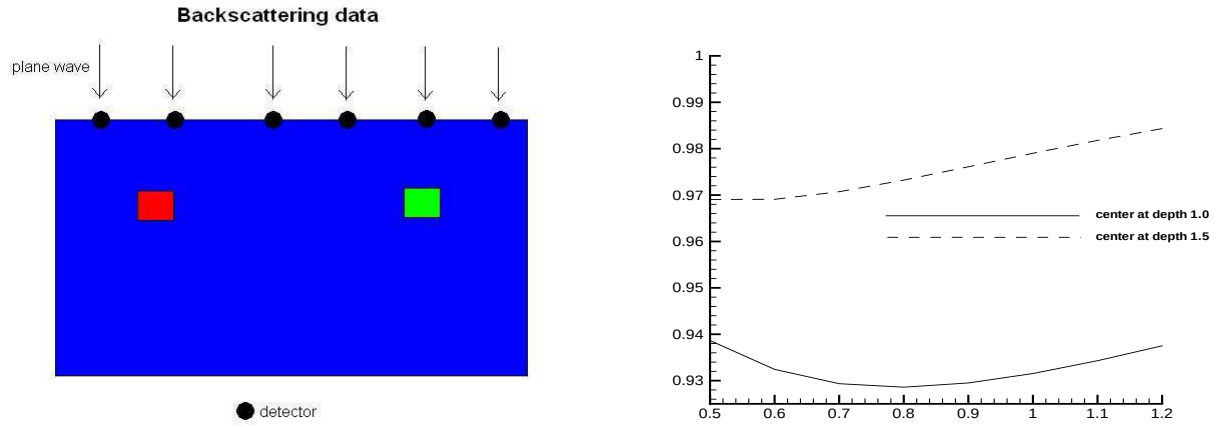

a) b)

Figure 1: *a) The schematic diagram of our data collection. The plane wave falls from the top and backscattering data are collected at the top side of this rectangle. b) The "sensitivity" function* $f(s) = w(0,0,s)/w_0(0,s)$, $s \in [0.5, 1.2]$ *for two different centers* $(0,1)$ *and* $(0,1.5)$ *of mine-like targets, which correspond to 10 cm and 15 cm depths respectively.*

8.1 Some details of the numerical implementation of the globally convergent method

We have generated the data for $s \in [0.5, 1.2]$ with the grid step size $h = 0.1$ in the s direction. Since the grid step size in the s-direction is $h = 0.1$ for $s \in [0.5, 1.2]$, then $\beta = 0.7$ and $N = 7$. Also, we took the number of iterations with respect to the tail $m_1 = m_2 = ... = m_N := m = 10$, since we have numerically observed the stabilization of functions $q_{n,k}, \varepsilon_r^{(n,k)}, V_{n,k}$ at $k = 10$, also, see section 4. In our computations we have relaxed the smoothness assumption in the QRM via taking in (4.7) the H^2-norm instead of the H^5-norm, see the first Remark 4.1.

Based on the experience of some earlier works on the QRM [8, 14] for linear ill-posed Cauchy problems, we have implemented the QRM via the FDM. Indeed, the FDM has allowed in [14] to image sharp peaks. On the other hand, the FEM of [8] did not let to image such peaks. So, we have written both terms under signs of norms of (4.7) in the FDM form. Next, to minimize the functional (4.7), we have used the conjugate gradient method. It is important that the derivatives with respect to the values of the unknown function at

grid points should be calculated explicitly. This was done using the Kronecker symbol, see details in [14]. As soon as discrete values $\widetilde{\varepsilon}_r^{(n,k)}$ were computed, we have averaged each such value at the point (x_i, z_j) over nine (9) neighboring grid points, including the point (x_i, z_j) : to decrease the reconstruction error. The resulting discrete function was taken as $\varepsilon_r^{(n,k)}$.

We have used the 49×49 mesh in Ω. However, an attempt to use a finer 98×98 mesh led to a poor quality results. Most likely this is because the dimension of our above mentioned finite dimensional space was becoming too large, thus making it "almost" infinitely dimensional, which would require to use in (4.7) the H^5-norm instead of the H^2-norm, see the first Remark 4.1. The regularization parameter in (4.7) was taken $\alpha = 0.04$.

We have made several sweeps over the interval $s \in [0.5, 1.2]$ as follows. Suppose that on the first s-sweep we have computed the discrete function $\varepsilon_r^{(1)}(\mathbf{x}) := \varepsilon_r^{(N,10)}(\mathbf{x})$, which corresponds to the last s-subinterval $[s_N, s_{N-1}] = [0.5, 0.6]$. Hence, we have also computed the corresponding discrete tail function $V^{(1)}(\mathbf{x})$. Next, we return to the first $s-$interval $[s_1, \overline{s}] = [1.1, 1.2]$, set $V_{1,1}^{(2)}(\mathbf{x}) := V^{(1)}(\mathbf{x})$ and repeat the algorithm of section 4. We kept repeating these $s-$sweeps p times until either the stabilization has was observed, i.e.

$$\|\varepsilon_r^{(p)} - \varepsilon_r^{(p-1)}\| \leq 10^{-5} \tag{8.1}$$

or an "explosion" of the gradient of the functional $J_{n,k}^{\alpha}$ on the sweep number p took place. "Explosion" means that

$$\|\nabla J_{n,k}^{\alpha}(q_{n,k}^{(p)})\| \geq 10^5, \tag{8.2}$$

for any appropriate values of indices n, k. Here and below $\|\cdot\|$ is the discrete $L_2(\Omega)-$norm. The stopping criterion (8.2) corresponds well with one of backbone principles of the theory of ill-posed problems. According to this principle, the iteration number can serve as one of regularization parameters, see pages 156 and 157 of [10].

Suppose that either (8.1) or (8.2) takes place. Then we work with the function $\varepsilon_r^{(p)}$. First, as it is usually done in imaging, we apply a truncation procedure. In this procedure we truncate to unity 85% of the max $\left|\varepsilon_r^{(p)}(\mathbf{x})\right|$, see Figure 2. If we have several local maxima of $\left|\varepsilon_r^{(p)}(\mathbf{x})\right|$, then we apply the truncation procedure as follows. Let $\{\mathbf{x}_i\}_{i=1}^r \subset \Omega$ be points where those local maxima are achieved, and values of those maxima are respectively $\{a_i\}_{i=1}^r$. Consider certain circles $\{B(\mathbf{x}_i)\}_{i=1}^r \subset \Omega$ with the centers at points $\{\mathbf{x}_i\}_{i=1}^r$ and such that $\overline{B}(\mathbf{x}_i) \cap \overline{B}(\mathbf{x}_j) = \varnothing$ for $i \neq j$. In each circle $B(\mathbf{x}_i)$ set

$$\widetilde{\varepsilon}_r^{(p)}(\mathbf{x}) := \begin{cases} \varepsilon_r^{(p)}(\mathbf{x}) \text{ if } \left|\varepsilon_r^{(p)}(\mathbf{x})\right| \geq 0.85 a_i \\ 1, \text{ otherwise.} \end{cases}$$

Next, for all points $\mathbf{x} \in \Omega \diagdown \cup_{i=1}^r B(\mathbf{x}_i)$, we set $\widetilde{\varepsilon}_r^{(p)}(\mathbf{x}) := 1$. As a result, we have obtained the truncated function $\widetilde{\varepsilon}_r^{(p)}(\mathbf{x})$. Finally we set $\varepsilon_r^{glob}(\mathbf{x}) := \widetilde{\varepsilon}_r^{(p)}(\mathbf{x})$ and go to Stage 2.

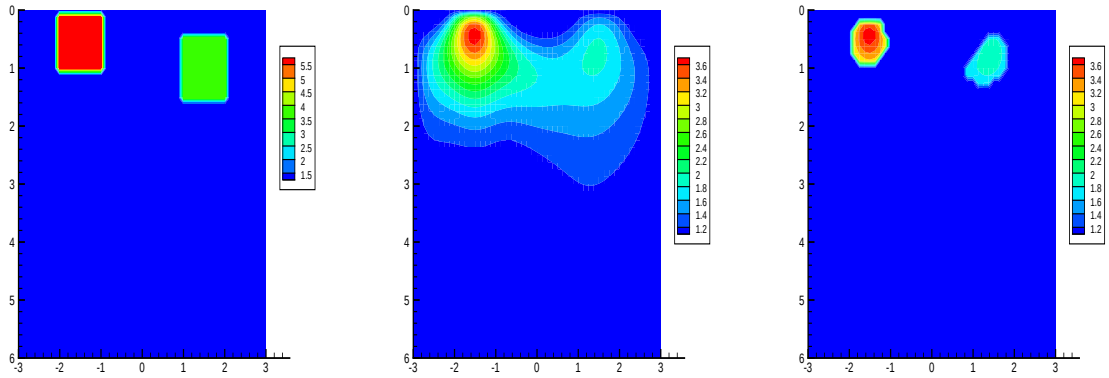

a) b) c)

Figure 2: *A typical example of the image resulting from the globally convergent stage. The rectangle is the domain* Ω. *This is the image of Test 1 (subsection 7.3). a) The correct coefficient. Inclusions are two squares with the same size* $d = 1$ *of their sides, which corresponds to 10 cm in real dimensions. In the left square* $\varepsilon_r = 6$, *in the right one* $\varepsilon_r = 4$ *and* $\varepsilon_r = 1$ *everywhere else, see (7.5) and (7.6). However, we do not assume knowledge of* $\varepsilon_r(\mathbf{x})$ *in* Ω. *Centers of these squares are at* $(x_1^*, z_1^*) = (-1.5, 0.4)$ *and* $(x_2^*, z_2^*) = (1.5, 1.0)$. *b) The computed coefficient before truncation. Locations of targets are judged by two local maxima. So, locations are imaged accurately. However, the error of the computed values of the coefficient* ε_r *in them is about 40%. c) The image of b) after the truncation procedure, see the text.*

8.2 The second stage of our two-stage numerical procedure: a modified gradient method

Recall that this method is used on the second stage of our two-stage numerical procedure. Since this method is secondary to us and since we want to save space, we derive a modified gradient method only briefly here. A complete, although space consuming derivation, including the rigorous derivation of Frechét derivatives, can be done using the framework developed in [3, 4]. We call our technique the "modified gradient method" because rather than following usual steps of the gradient method, we find zero of the Fréchet derivative of the Tikhonov functional via solving an equation with a contractual mapping operator.

Consider a wider rectangle $\Omega' \supset \Omega$, where $\Omega' = (-4, 4) \times (0, 6)$. We assume that both Dirichlet φ_0 and Neumann φ_1 boundary conditions are given on a wider interval $\Gamma_1' = \{z = 0\} \cap \overline{\Omega}'$, $\Gamma_1 \subset\subset \Gamma_1'$, i.e. similarly with (2.11)

$$\widetilde{w}(\mathbf{x}, s)|_{\Gamma_1'} = \widetilde{\varphi}_0(x, s), \tag{8.3}$$

$$\widetilde{w}_z(\mathbf{x}, s)|_{\Gamma_1'} = \widetilde{\varphi}_1(x, s) + e^{-s|z_0|}. \tag{8.4}$$

Also, we have observed in our computations that $\lim_{|\mathbf{x}|\to\infty} |\nabla \widetilde{w}(\mathbf{x}, s)| = 0$. Hence, we use

$$\partial_n \widetilde{w}_x \,|_{\partial\Omega' \setminus \Gamma_1'} = 0. \tag{8.5}$$

In addition, by (7.3)

$$\Delta\widetilde{w} - s^2\varepsilon_r(\mathbf{x})\widetilde{w} - s^2(\varepsilon_r(\mathbf{x}) - 1)w_0(z,s) = 0, \text{ in } \Omega'. \tag{8.6}$$

So, we now consider the solution of the boundary value problem (8.4)-(8.6), keeping the same notation. We want to find such a coefficient $\varepsilon_r(\mathbf{x})$, which would minimize the following Tikhonov functional

$$\begin{aligned} T(\varepsilon_r) &= \frac{1}{2}\int\limits_a^b \int\limits_{\Gamma_1'} (\widetilde{w}(x,0,s) - \widetilde{\varphi}_0(x,s))^2 dxds + \frac{\theta}{2}\left\|\varepsilon_r - \varepsilon_r^{glob}\right\|^2_{L_2(\Omega)} \\ &+ \int\limits_a^b \int\limits_{\Omega'} \lambda[\Delta\widetilde{w} - s^2\varepsilon_r(\mathbf{x})\widetilde{w} - s^2(\varepsilon_r(\mathbf{x}) - 1)w_0(z,s)]d\mathbf{x}ds, \end{aligned} \tag{8.7}$$

where $\theta > 0$ is the regularization parameter and $\lambda(\mathbf{x}, s)$ is the solution of the so-called "adjoint problem",

$$\Delta\lambda - s^2\varepsilon_r(\mathbf{x})\lambda = 0, \text{ in } \Omega', \tag{8.8}$$

$$\lambda_z(x,0,s) = \widetilde{w}(x,0,s) - \varphi_0(x,s),\ \partial_n\lambda|_{\partial\Omega' \setminus \Gamma_1'} = 0. \tag{8.9}$$

If the coefficient $\varepsilon_r(\mathbf{x})$ is such that, in addition to (8.4)-(8.6), (8.3) is true, then $T(\varepsilon_r) = 0$, i.e. this coefficient provides the minimum value for the functional T. Because of (8.8), the second line in (8.7) equals zero. Although boundary value problems (8.4)-(8.6) and (8.8), (8.9) are considered in the domain Ω' with a non-smooth boundary, a discussion about existence of their solutions is outside of the scope of this paper. We have always observed existence of numerical solutions with no singularities in our computations. Although, by the Tikhonov theory, one should consider a stronger H^k-norm of $\varepsilon_r - \varepsilon_r^{glob}$ in (8.7) [18], we have found in our computations that the simpler L_2-norm is sufficient. This is likely because we have worked computationally worked with not too many grid points. Using the framework of [3, 4], one can derive the following expression for the Fréchet derivative $T'(\varepsilon_r)$ of the functional T

$$T'(\varepsilon_r)(\mathbf{x}) = \theta\left(\varepsilon_r - \varepsilon_r^{glob}\right)(\mathbf{x}) - \int\limits_a^b s^2\left[\lambda(\widetilde{w} + w_0)\right](\mathbf{x}, s)\, ds, \mathbf{x} \in \Omega.$$

Hence, to find a minimizer, one should solve the equation $T'(\varepsilon_r) = 0$. We solve it iteratively as follows

$$\varepsilon_r^n(\mathbf{x}) = \varepsilon_r^{glob}(\mathbf{x}) + \frac{1}{\theta}\int\limits_a^b s^2\left[\lambda(\widetilde{w} + w_0)\right](\mathbf{x}, s, \varepsilon_r^{n-1})ds, \mathbf{x} \in \Omega, \tag{8.10}$$

where functions $\widetilde{w}(\mathbf{x}, s, \varepsilon_r^{n-1})$ and $\lambda(\mathbf{x}, s, \varepsilon_r^{n-1})$ are solutions of problems (8.4)-(8.6) and (8.8), (8.9) respectively with $\varepsilon_r(\mathbf{x}) := \varepsilon_r^{n-1}(\mathbf{x})$. One can easily prove that one can choose the number $(b-a)/\theta$ so small that the operator in (8.10) is contractual mapping. We have worked with such an operator in our computations. We have iterated in (8.10) until the stabilization has occurred, i.e. we have stopped iterations as soon as $\|\varepsilon_r^n - \varepsilon_r^{n-1}\|/\|\varepsilon_r^{n-1}\| \leq 10^{-5}$, where $\|\cdot\|$ is the discrete $L_2(\Omega)$ norm. Then we set that our computed solution is $\varepsilon_r^n(\mathbf{x})$. In our computations we took $a = 0.01, b = 0.05, \theta = 0.15$.

8.3 Numerical results

In our numerical tests we have introduced the multiplicative random noise in the boundary data using the following expression

$$w_\sigma(x_i, 0, s_j) = w(x_i, 0, s_j)[1 + \varsigma\sigma], \ i = 0, ..., M; \ , j = 1, .., N,$$

where $w(x_i, 0, s_j)$ is the value of the computationally simulated function w at the grid point $(x_i, 0) \in \Gamma_1'$ and at the value $s := s_j$ of the pseudo frequency, ς is a random number in the interval $[-1; 1]$ with the uniform distribution, and $\sigma = 0.05$ is the noise level. Hence, the random error is presented only in Dirichlet data but not in Neumann data.

Test 1. We test our numerical method for the case of two squares with the same size $d = 1$ of their sides. In the left square $\varepsilon_r = 6$, in the right one $\varepsilon_r = 4$ and $\varepsilon_r = 1$ everywhere else, see (7.6). Centers of these squares are at $(x_1^*, z_1^*) = (-1.5, 0.4)$ and $(x_2^*, z_2^*) = (1.5, 1.0)$. However, we do not assume *a priori* in our algorithm neither the presence of these squares nor a knowledge of $\varepsilon_r(\mathbf{x})$ at any point of the rectangle Ω. See Figure 2 for the globally convergent stage and Figure 3 for the final result.

Test 2. Consider now the case of imaging of a piece of wood, see (7.6). So, now our target is a square with the $d = 1$ size of its side. Inside of this square $\varepsilon_r = 0.5 < 1$ and $\varepsilon_r = 1$ outside. Figure 4 displays both this square and the reconstruction result.

Acknowledgments

This work was supported by the U.S. Army Research Laboratory and U.S. ArmyF Research Office under grants number W911NF-08-1-0470 and W911NF-09-1–0409 as well as by the Russian Foundation for Basic Research under the grant number 08-01-00312.

References

[1] L. Beilina and M. V. Klibanov, *A globally convergent numerical method for a coefficient inverse problem*, SIAM J. Sci. Comp., 31 (2008), pp. 478-509.

[2] L. Beilina and M. V. Klibanov, *Synthesis of global convergence and adaptivity for a hyperbolic coefficient inverse problem in 3D*, J. Inverse and Ill-Posed Problems, 18 (2010), pp. 85-132.

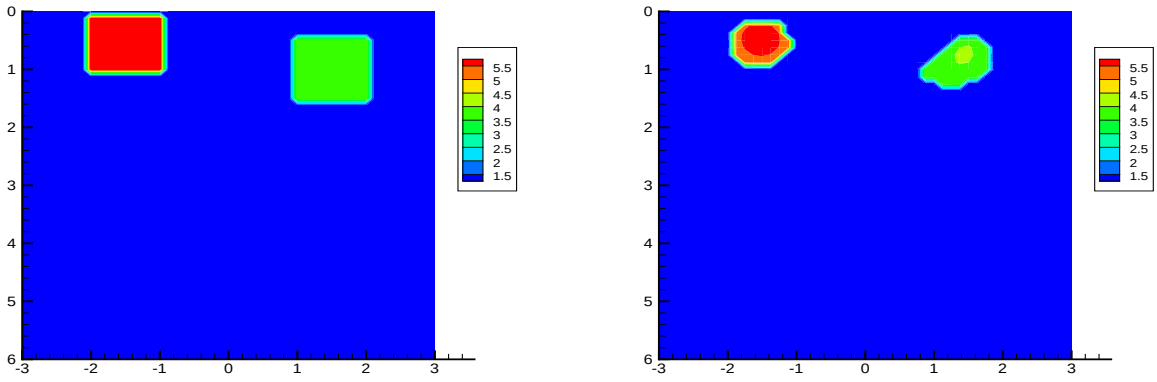

Figure 3: *Test 1. The image obtained on the globally convergent stage is displayed on Fig. 2-c). a) The correct image. Centers of small squares are at* $(x_1^*, z_1^*) = (-1.5, 0.4)$ *and* $(x_2^*, z_2^*) = (1.5, 1.0)$ *and values of the target coefficient are* $\varepsilon_r = 6$ *in the left square,* $\varepsilon_r = 4$ *in the right square and* $\varepsilon_r = 1$ *everywhere else. b) The imaged coefficient* $\varepsilon_r(\mathbf{x})$ *resulting of our two-stage numerical procedure. Both locations of centers of targets and values of* $\varepsilon_r(x)$ *at those centers are imaged accurately. We have not used truncation on the second stage.*

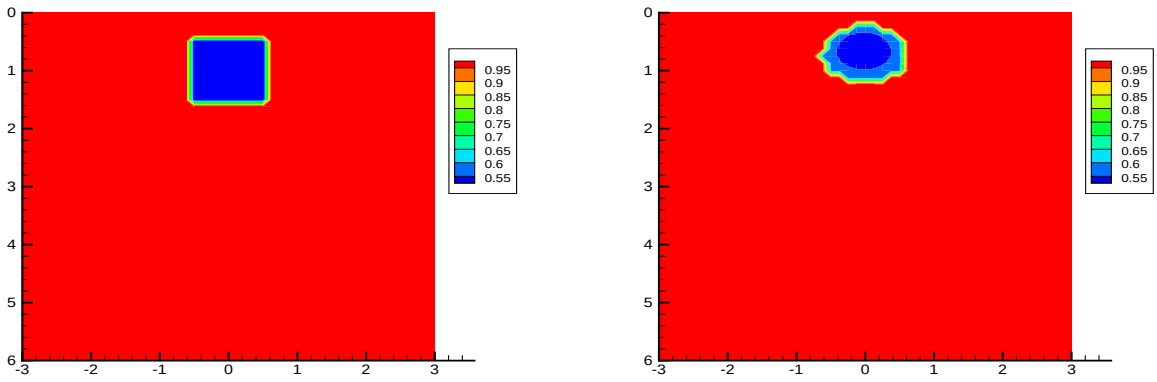

Figure 4: *Test 2. Imaging of a wooden-like targets: small square with the length of its side* $d = 1$*, see a). Inside of this small square* $_r = 0.5$ *and* $\varepsilon_r = 1$ *outside of it.However, neither the presence of the small square nor the value of the unknown coefficient* $\varepsilon_r(x)$ *at any point of this rectangle* Ω *are not assumed to be known a priori in our algorithm. b) The image computed after the two-stage numerical procedure. Location of the center of the small square and the value of* $\varepsilon_r = 0.5$ *at that center are imaged accurately. The value* $\varepsilon_r = 1$ *outside of the imaged small square is also accurately imaged.*

[3] L. Beilina and M. V. Klibanov, *A posteriori error estimates for the adaptivity technique for the Tikhonov functional and global convergence for a coefficient inverse problem,* Inverse Problems, 26 (2010), 045012.

[4] L. Beilina, M. V. Klibanov and M.Yu. Kokurin, *Adaptivity with relaxation for ill-posed problems and global convergence for a coefficient inverse problem*, J. Mathematical Sciences, 167 (2010), No. 3, pp. 279-325.

[5] L. Bourgeois, *A mixed formulation of quasi-reversibility to solve the Cauchy problem for Laplace's equation*, Inverse Problems, 21 (2005), pp. 1087–1104.

[6] L. Bourgeois, *Convergence rates for the quasi-reversibility method to solve the Cauchy problem for Laplace's equation*, Inverse Problems, 22 (2006), pp. 413–430.

[7] M. Cheney and D. Isaacson, *Inverse problems for a perturbed dissipative half-space*, Inverse Problems, 11 (1995), pp. 865-888.

[8] C. Clason and M.V. Klibanov, *The quasi-reversibility method for thermoacoustic tomography in a heterogeneous medium*, SIAM J. Sci. Comp., 30 (2007), pp. 1-23.

[9] B.A. Dubrovin, S.P. Novikov and A.T. Fomenko, *Modern Geometry Methods and Applications*, Springer-Verlag, Berlin, 1985.

[10] H.W. Engl, M. Hanke and A. Neubauer, *Regularization of Inverse Problems*, Kluwer Academic Publishers, Boston, 2000.

[11] D. Gilbarg and N.S. Trudinger, *Elliptic Partial Differential Equations of Second Order*, Springer-Verlag, Berlin, 1983.

[12] M.V. Klibanov, M.A Fiddy, L. Beilina, N. Pantong and J. Schenk, *Picosecond scale experimental verification of a globally convergent algorithm for a coefficient inverse problem,* Inverse Problems, 26 (2010), 045003.

[13] M.V. Klibanov and A. Timonov, *Carleman Estimates for Coefficient Inverse Problems and Numerical Applications*, VPS, The Netherlands, 2004.

[14] M.V. Klibanov, A.V. Kuzhuget, S.I. Kabanikhin and D.V. Nechaev, *A new version of the quasi-reversibility method for the thermoacoustic tomography and a coefficient inverse problem*, Applicable Analysis, 87 (2008), pp. 1227-1254.

[15] R. Lattes and J.-L. Lions, *The Method of Quasireversibility: Applications to Partial Differential Equation*s, Elsevier, New York, 1969.

[16] M.M. Lavrent'ev, V.G. Romanov and S.P. Shishatskii, *Ill-Posed Problems of Mathematical Physics and Analysis*, AMS, Providence, RI, 1986.

[17] V.G. Romanov and M. Yamamoto, *Recovering a Lamé kernel in a viscoelastiv equation by a single boundary measurement*, Applicable Analysis, 89 (2010), pp. 377-390.

[18] A.N. Tikhonov, A.V. Goncharsky, V.V. Stepanov and A.G. Yagola, *Numerical Methods for Solutions of Ill-Posed Problems,* Kluwer, London, 1995.